

U.S. DEPARTMENT OF THE INTERIOR

U.S. GEOLOGICAL SURVEY



APPLICATION OF PATTERN RECOGNITION METHOD (PRM)
TO ESTIMATE GROUND MOTIONS
IN SAN FRANCISCO PENINSULA, CALIFORNIA

M. Çelebi
U.S. Geological Survey
345 Middlefield Road
Menlo Park, CA 94025-3591

A. Gorshkov and M. Filimonov
International Institute of Earthquake Prediction
Theory and Mathematical Geophysics
Academy of Sciences
Warshavskoye sh.79, k.2
113556 Moscow, Russia

OPEN-FILE REPORT 93-398

This report is preliminary and has not been reviewed for conformity with U.S. Geological Survey editorial standards or with the North American Stratigraphic Code. Any use of trade, product, or firm names is for descriptive purposes only and does not imply endorsement by the USGS.

December 1, 1993

U.S. DEPARTMENT OF THE INTERIOR

U.S. GEOLOGICAL SURVEY

**APPLICATION OF PATTERN RECOGNITION METHOD (PRM)
TO ESTIMATE GROUND MOTIONS
IN SAN FRANCISCO PENINSULA, CALIFORNIA**

**M. Çelebi
U.S. Geological Survey
345 Middlefield Road
Menlo Park, CA 94025-3591**

**A. Gorshkov and M. Filimonov
International Institute of Earthquake Prediction
Theory and Mathematical Geophysics
Academy of Sciences
Warshavskoye sh.79, k.2
113556 Moscow, Russia**

OPEN-FILE REPORT 93-398

This report is preliminary and has not been reviewed for conformity with U.S. Geological Survey editorial standards or with the North American Stratigraphic Code. Any use of trade, product, or firm names is for descriptive purposes only and does not imply endorsement by the USGS.

December 1, 1993

CONTENTS

	Page No.
ACKNOWLEDGMENTS	ii
I. INTRODUCTION	1
II. DESCRIPTION OF THE PATTERN RECOGNITION METHOD	2
III. COMPILATION OF REQUISITE DATA	5
III.1. Strong-Motion Data	5
III.2. Topographic Parameters	6
III.3. Geological Parameters	6
III.4. Other Parameters	7
IV. APPLICATION	7
IV.1. Formulation of the Problem	7
IV.2. Selection of Learning Set (W_0)	8
IV.3. Parameters of the Elements	8
IV.4. Discretization and Coding	9
IV.5. Learning Stage.	9
IV.6. Recognition Stage.	9
IV.7. Evaluation of the Reliability of Characteristic Traits.	10
V. DISCUSSION AND CONCLUSIONS	11
REFERENCES	14
TABLES	17
FIGURES	30

ACKNOWLEDGMENTS

The authors gratefully acknowledge the in-depth discussions and suggestions provided by Dr. Alexei Tumarkin, University of California, Santa Barbara, California. The authors thank Ray Eis and Emmett Dingel for drafting, Howard Bundock for computer help, and Carol Sullivan for editing/typing. The authors also thank Cheryl Eichorn, USGS, Reston, VA., Muriel Jacobson and Barbara Simpson for all the assistance provided during the two month stay of the visitors. This study has been carried out in the framework of the U.S.–Russian Agreement on Cooperation in the Field of Environmental Protection (Area IX—Earthquake Prediction, 02.09–14) between August 2–September 29, 1993.

I. INTRODUCTION

The severity of shaking at a given location during an earthquake depends on many factors including but not limited to the magnitude of the earthquake, distance to the rupture zone, and local site conditions. Within the last decade, the effects of local site conditions on ground motion and on the resulting severity and distribution of damage has been demonstrated by observed damage and instrumental data from the 1985 Michoacan, Mexico ($M_s = 8.1$), the 1988 Armenian ($M_s = 7.0$), the 1989 Loma Prieta, California ($M_s = 7.1$) and other earthquakes. The effects of site conditions on characteristics of strong motions have been intensively studied (Borcherdt and Gibbs, 1976; Shiga *et al.*, 1979; Davis *et al.*, 1983; Geli *et al.*, 1988; Çelebi, 1987, 1991). Future and more effective identification of requisite site characteristics for improved estimation of ground motion is an important objective of earthquake hazard reduction processes. The influence of site characteristics on the amplification of ground motion is better understood now than approximately 20 years ago, due to the increase in recorded strong motion data during recent earthquakes and extensive efforts to define site conditions.

This study is an attempt to identify some site characteristics that influenced the degree of ground motion amplification during the Loma Prieta earthquake (LPE) by using pattern recognition method (PRM). Part of the San Francisco peninsula is adopted as a pilot study area using PRM. The main reason for selecting this area is the availability of geological and seismological data. Taking into account the high-density urban population of the San Francisco Bay area, results of such a study can be used to improve existing seismic zonation maps; thus, reducing earthquake hazards.

The area covered in this study includes San Francisco and the San Francisco peninsula, extending south to Monterey Bay and is approximately 100-km long and 40-km wide, between the Pacific Coast and Highway 101 in the Santa Clara basin. The general outline of the area is shown by the grids (marked 1 thru 133) in Figure 1. The elements marked 134 thru 140 in the East Bay, outside of the main study area, are test elements as described in Section IV.

The topography of the area is best described by a system of roughly parallel ridges, part of the Santa Cruz Mountains and by the flat areas of the Santa Clara basin. Peak

elevation of the Santa Cruz Mountains in the SE direction reaches 1240 m. (3791 ft.) at Loma Prieta. Most ridges are characterized by very steep slopes. In the northern part of the area, low-elevated hills are predominant.

Geology of the area is very complicated. The Santa Cruz Mountains consist mainly of intensively deformed Mesozoic–Cenozoic marine metasedimentary rocks heavily dissected by a system of faults. The well-known San Andreas fault runs over the study area in a nominally NW–SE direction. Mountain ridges are predominantly composed of sandstones, mudstones, shales, limestones, conglomerates and other noncrystalline rocks. Young sedimentary deposits that filled up the Santa Clara basin are represented by soft, unconsolidated alluvium and mud. In general, the topographic and geological environment of the area is an important influence on the degree of shaking during an earthquake.

The purpose of this study is to apply the pattern recognition method to the San Francisco peninsula and immediate vicinity affected by the Loma Prieta earthquake. It is a limited study carried out in a short time frame mainly to demonstrate the application of PRM to San Francisco Bay area. Further refinements of this application with improved and extended data base will be necessary to achieve better results. As a by-product of this study, it is desired to identify by PRM those significant site-related parameters that influence earthquake ground motions that cause hazards in the area.

II. DESCRIPTION OF THE PATTERN RECOGNITION METHOD

Pattern recognition method (PRM) has been applied in geophysical investigations to identify earthquake prone areas for more than 20 years (Gelfand *et al.*, 1972, 1976, Bhatia *et al.*, 1992, and Gvishiani *et al.*, 1988). The method is based on a defined set of objects (referred to as “elements” in this study) of recognition. The software used in carrying out PRM algorithm, CORA-3, is developed by staff of the International Institute of Earthquake Prediction Theory and Mathematical Geophysics, Academy of Sciences, Russia.

The following definitions and symbols are used to better describe the algorithm:

- W = the general set of objects (or “elements” in this report) of recognition.

- $W_0 = (D_0, N_0)$ represents the learning set. $D_0 =$ positive elements (with strong potential to amplify) and $N_0 =$ negative elements.
- $\Pi : W = D \sqcup N$ represents a classification of W with algorithm Π ; *i.e.*, $\Pi : W = D \sqcup N$ to be a division of W into two subsets D and N such that $D \cup N = W$ and $D \cap N = 0$.
- $B_p = \{0, 1\}^p$ represents the binary space of p dimensions.
- $D : W \rightarrow B_p$ represents the binary description of objects, for each $w \in W : d(w) = \omega = (\omega_1, \dots, \omega_i, \dots, \omega_p)$, $w_i = 0$ or 1 .

In general, pattern recognition method requires the following steps:

- a) Selection of area of study.
- b) Determination of the elements (or objects) of recognition (W).
- c) Compilation of learning material set W_0 (D_0 and N_0).
- d) Parameterization of elements.
- e) Discretization and coding of values of parameters.
- f) Running of pattern recognition algorithm in order to obtain classification of elements: $W = D \sqcup N$.
- g) Evaluation of the reliability of characteristic traits.
- h) Interpretation of the results.

The algorithm has two main stages: (1) the learning stage and (2) the classification stage. During the learning stage, the input data that is assigned to describe the parameters of the elements in the learning set, W_0 , are used in order to generate characteristic traits of each class D_0 and N_0 . In general, the feature is a triple binary combination which frequently appears on elements of one class but rarely appears on elements of contrary class when the elements are represented in binary form after discretization.

The algorithm CORA-3 characterizes the D objects and N objects by *traits*, that is, by some combination of values of the components of the binary vector representing

the object in B space. This is a way to represent the joint occurrence of some physical properties and the traits are defined in the form of a matrix:

$$T = \begin{vmatrix} i_1 & i_2 & i_3 \\ \alpha_1 & \alpha_2 & \alpha_3 \end{vmatrix}$$

where $i_r = 1, 2, \dots, p$; $\alpha_r = 0$ or 1 ; $r = 1, 2, 3$.

An object $w \in W$ possesses the feature T if $w_{i_r} = \alpha_r$, for its description $d(w)$ in binary space B_p . Let $K_{D_0}(T)$ be the number of objects of class D_0 and $K_{N_0}(T)$ number of object of class N_0 possessing the same feature. Let $K_D, \tilde{K}_D, K_N, \tilde{K}_N$ be some fixed integers, free parameters of the algorithm. The feature T is considered to be a characteristic D -feature if

$$K_{D_0}(T) \geq K_D \text{ and } K_{N_0}(T) \leq \tilde{K}_D.$$

It is a characteristic N -feature if

$$K_{N_0}(T) \geq K_N \text{ and } K_{D_0}(T) \leq \tilde{K}_N.$$

During the second stage of the algorithm, classification is realized based on the following criteria. For each $w \in W$ we define $\Delta(w) = N_D(w) - N_N(w)$ where $N_x(w)$ is the number of traits which appear in the object w . Let Δ_t be an additional free parameter. The classification $C(W_0, K_D, \tilde{K}_D, K_N, \tilde{K}_N, \Delta_t) : W = D \sqcup N$ is defined as:

$$D = \{w \in W : \Delta(w) \geq \Delta_t\}$$

$$N = \{w \in W : \Delta(w) < \Delta_t\}$$

Each element of recognition is described by a set of real parameters. In order to apply pattern recognition algorithm, all parameters describing the elements have to be discretized and coded in binary form. The procedure of discretization includes also setting thresholds of discretization of each parameter, which subdivide the interval of altering of this parameter into several parts. In most cases, the thresholds are adjusted automatically in order for all intervals to get approximately an equal number of elements. To each interval, a unique binary combination is assigned. The algorithm searches the interval

to which the value of the current parameter belongs. Then, real value is substituted by the binary code corresponding to this interval. After all elements are coded, the pattern recognition algorithm is applied.

III. COMPILATION OF REQUISITE DATA

The Pattern Recognition Method (PRM) is used in this study to identify the sites that amplify earthquake ground motions within the San Francisco peninsula. To apply this method, the study area was gridded into 133 squares ($5 \text{ km} \times 5 \text{ km}$), each of which is considered an element of recognition.

The Bay Area is probably the best-studied region on the globe from a geologic and seismologic point of view. A considerable amount of data exists in digital and mapped form and is easily available to users. In this study, all available data within the area of investigation are used. The data used can be put into three categories:

- (a) strong motion data;
- (b) topographic data;
- (c) geological data.

Accordingly, the list of parameters (Table 1) intended for testing in this study has been worked out on the basis of the available data.

III.1. Strong-Motion Data

The strong-motion data used in this study was compiled from a number of reports related to the 1989 Loma Prieta earthquake (EERI, 1990, Shakal *et al.*, 1989).

We used peak ground accelerations recorded by two different networks of strong-motion stations operated by the U.S. Geological Survey and the California Strong Motion Instrumentation Program (CSMIP) of the State of California. Eleven USGS and 27 CSMIP stations are located within the investigation area. The names of these stations and recorded peak horizontal ground accelerations are presented in Table 2. We have adopted data from free-field stations and from basements of 1- and 2-story buildings. It must be emphasized that strong motion data were used only as an input to develop the learning set of PRM.

III.2. Topographic Parameters

In order to identify the role of topography in amplification, six topographic parameters were selected. These are: (1) maximum elevation within the element, (2) minimum elevation within the element, (3) elevation difference between points of maximum and minimum elevation, (4) distance between points of maximum and minimum elevation, (5) slope or gradient, and (6) predominant landforms. Particular values of parameters 1–5 within each element were taken from the 1:125,000 scale topographic map of the San Francisco Bay region. Parameter 5, slope, was defined as a ratio of elevation difference to the distance between the highest and lowest points. This ratio characterizes general slope of the surface within the element.

Predominant landforms were also extracted from the above map. Five basic landforms or their combinations are distinguished in the area under study. These are: ridges, slope of the ridges, flat areas, hills, and combination of slopes with flat areas. Hills are characteristic for a number of elements located in the northern part of the Peninsula occupied by the city of San Francisco, as well as for some elements between the San Andreas fault and San Francisco Bay. Topography is considered to be important for an element if there is a ridge covering most of the area of an element. Most elements in the Santa Cruz Mountains therefore had topography as a parameter. The majority of elements for which topography was defined with a slope were located in this mountain area. Elements with a flat surface were concentrated around the San Francisco Bay and in the Santa Clara basin. Of course, the suggested characterization of the topography is very crude but for this preliminary testing of the method, it appears to be satisfactory.

III.3. Geological Parameters

In this study, only one type of geological information was used. To characterize site conditions, we used information on soil conditions extracted from the map entitled “The effect of soil type on earthquake risk” (Hall). On this map, four soil types are designated: (a) stable rock, (b) unstable rock, (c) unconsolidated soil, and (d) mud and fill. If an element contains more than one soil type, then, the soil parameter for that particular

element was defined by the type of soil that extends to more than 50% of the whole square area.

This soil type classification seems to be reasonable to study geological amplification and also can be related to the current trends in various codes. It is doubtless that other geological factors such as the depth of soil to bedrock and slope of bedrock-surface can cause ground motion amplification. Unfortunately, this data is not available for the entire study area. This geotechnical information in general exists only for some sites where strong-motion instruments were stationed.

III.4. Other Parameters

Apart from geological and topographic environments, the intensity of strong motion at each particular site is closely connected with the distance and azimuth to the epicenter. That is why azimuth to the epicenter was also included in the list of parameters. Instead of the distance to the epicenter, we considered the distance to the rupture zone. This data was extracted from the special issue of Earthquake Spectra (Earthquake Spectra, 1990).

Based on previous results using theoretical modeling (Boore, 1987), we tried to estimate the possible influence of the San Andreas fault on ground motion amplification. For this purpose, the distance from the center of each element to the San Andreas fault was taken into consideration.

IV. APPLICATION

IV.1 Formulation of the problem

In Figure 2, it is shown that, for LPE, the recorded PGA decreases with epicentral distance, an outcome of attenuation law concerning earthquake motions. However, in the case of LPE, a number of distant stations recorded amplified ground motions with high PGA values (see Table 2).

It is therefore important to determine whether ground motions at sites, that were not instrumented, amplified. To answer this question, the use of recorded PGA values is difficult because of the attenuation of (peak) accelerations with epicentral distance (DEP). In order to eliminate the effect of DEP, in this study, instead of PGA, we adopt, PGA_1 ,

according to geometrical spreading factor $1/DEP$ (Aki and Richards, 1980), defined as follows:

$$PGA_1 = PGA \times (DEP)$$

Large PGA_1 values correspond to sites where recorded PGA values are not in agreement with attenuation law and consequently amplification of ground motions can be expected. Based on this assumption, the goal of recognition is to classify the whole set of elements in the study area into two classes: (1) positive elements (D) indicating that in those elements, strong site amplification occurs, and (2) negative elements (N) indicating that in those elements, site amplification is weak or does not occur. The criteria for D or N is the threshold PGA_0 , yet to be defined. In this study, PGA_0 is the threshold median value of PGA_1 for the elements from W_o .

IV.2. Selection of Learning Sets (W_o)

Of the total number of 133 elements, 29 elements contained strong-motion stations that recorded the Loma Prieta earthquake. The 38 peak values of accelerations recorded at these 29 stations are tabulated in Table 2. When, at one element, more than one station recorded the earthquake, the largest peak acceleration within the element is adopted. The 29 elements used as learning set, W_o , are: 1, 2, 3, 4, 5, 6, 7, 8, 11, 14, 21, 23, 27, 33, 34, 36, 43, 44, 45, 47, 48, 49, 58, 74, 85, 88, 126, 129 and 130 (See Figure 1).

We subdivided the learning set (W_o) into two sets (D_o and N_o), using the threshold PGA_0 equal to 9.22 which is the median value of PGA_1 of set W_o (Figure 3). It is obvious that this PGA_0 value corresponds to the 0.922 g PGA value at an element, if this element is 10 km away from the epicenter. A total of 14 elements (1, 3, 4, 6, 7, 8, 14, 23, 27, 36, 44, 45, 47 and 85) were accepted as learning set D_o of class D because they fall above $PGA_0 = 9.22$. The remaining 15 elements with $PGA_1 < 9.22$ (2, 4, 5, 11, 21, 33, 34, 43, 48, 49, 58, 88, 126, 129, 130) were put into learning set N_o for N class (see Figure 3).

IV.3. Parameters of the Elements

Elements are described by 3 groups of parameters summarized in Table 1. The variation of each parameter against peak acceleration is shown in Figures 4 thru 13. The following parameters were found to be significant to evaluate D_0 and N_0 elements: Azimuth (A_z), H_{\min} , H_{\max} , ΔH , DSF , Gradient ($\Delta H/L$), Topography, Soil Type.

IV.4. Discretization and Coding

The parameters of the elements were discretized and the elements were coded by binary vectors. The thresholds of discretization for each parameter are given in Table 1. Parameters were coded in two ways. In the first way the interval of parameter is subdivided into two or three intervals. Each value of the parameter is coded by binary combination, depending on the interval (see Table 1). In the second, each value of the parameter corresponds to a certain binary combination. As a result, all elements of recognition were represented by 19-component binary vectors (*See Table 8*).

IV.5. Learning Stage

On the basis of learning set, two sets of traits which are characteristic for D_0 - and N_0 -classes, respectively, were selected by ‘‘COR-3’’ algorithm. These are given in Table 3. The following thresholds for selection and rejection were used for the selection of characteristic traits:

$$K_D = 8, \tilde{K}_D = 5, K_N = 9, \tilde{K}_N = 4.$$

IV.6. Recognition Stage

The elements from learning set and examination set were classified according to the following rule. An element was assigned to D -class if $(Nd - Nn)$ was greater or equal to 1; otherwise, it was assigned to class N . As a result, 9 out of 14 elements originally from the D_0 class were classified as D (1, 3, 6, 8, 14, 23, 36, 45 and 74). Four elements (7, 27, 47, 85) originally from the D_0 class were classified as N and three elements (2, 4, 5) from the N_0 class were classified as D . In Figure 3, it is observed that these elements are located very close to the formal median threshold (mean $PGA_1 = 9,22$) for D_0 and N_0 classes.

Apparently the elements situated around the median are uncertain and could be referred to both of the classes D_0 and N_0 at the stage of learning.

In total, 31 objects among 133 defined in San Francisco peninsula were recognized to be positive (those with possible site ground motion amplification effect during the LPE with $M = 7.1$). These elements are identified in Figure 14.

IV.7. Evaluation of the Reliability of Characteristic Traits

In order to determine the reliability of the characteristic traits of this study, we carried out the following control experiment. We considered 7 more elements with available values of peak ground motion acceleration. These elements (134, 135, 136, 137, 138, 139 and 140) are in the San Francisco Bar Area and are also located in Figure 1 but are out of our grid. PGA values, Loma Prieta epicentral distance and PGA_1 values for these elements are listed in Table 5. The fact that amplifications of ground motions occurred during the LPE within elements 134 and 135 is well publicized. Within elements 136, 138 and 139, recorded PGA values, in general, are in agreement with natural attenuation; hence, most likely, ground motions did not amplify at these sites. Actually, apriori, we know in which elements amplification occurred. That is why these elements were selected for testing. However, the principal question is whether characteristic traits based only on geologic and topographic data are sufficient requisites to identify those sites where amplification occurred.

To answer this question, we consider the above mentioned seven elements which have not been used in learning and recognition stages. For all these patterns, values of initial parameters were evaluated. These are summarized in Table 6. Next, characteristic traits from Table 3 were applied in order to determine the number of traits of each class (D or N) in each of the test elements. The number of D-traits and N-traits for each test element is given in Table 7. In accordance with classification rule in Section IV.5, the element was assigned to be D-class if $Nd - Nn$ is greater or equal to 1; otherwise, we assign the element to class N . As a result, elements 134, 135 and 137 were recognized to belong to D class while elements 136, 138, 139 and 140 were assigned to N class. This result is in good agreement with observations and recorded PGA values (Table 5). Therefore, it may

be concluded that characteristic traits obtained in this study allow us to reliably identify particular sites where ground motions were amplified during LPE due to topographical and geological conditions.

V. DISCUSSION AND CONCLUSIONS

Analysis of post earthquake damage surveys and strong-motion data recorded during the Loma Prieta earthquake indicated the significant effects of local site conditions on the resulting damage patterns (USGS Staff, 1989,1990; EERI, 1989,1990). At several stations that recorded the earthquake, it was determined that ground motions were amplified due to by local site conditions. Some of the well known regions of the San Francisco Bay area where amplification occurred are: San Francisco's Marina District (Holzer and O'Rourke,1990), Cypress Street viaduct (Hough et al.,1990), Oakland (Hanks and Brady, 1991). According to results obtained in this study, ground motions generated by the Loma Prieta earthquake were amplified at a number of other sites within the Bay Area due to specific combinations of topographic and geological factors.

Let us consider in detail the loci of elements recognized to be positive (amplification-prone) with a special attention to their characteristic traits resulted from the recognition study conducted herein.

Characteristic traits selected by "CORA-3" algorithm both for the positive (amplification-prone) elements and negative elements are represented in Table 3. These traits identified seven parameters that turned out to be most significant among the initial eleven parameters for the creation of the decision rule (see Table 1). These significant parameters are: (a) maximum elevation, (b) minimum elevation, (c) difference between maximum and minimum elevations, (d) topographic gradient, (e) distance to San Andreas fault, (f) predominant landforms (topography), and (g) predominant soil type.

These parameters form the five characteristic traits for positive, (*D*), amplification-prone, and four negative, (*N*), non-prone elements.

In accordance with selected D traits, amplification-prone elements are generally characterized by gentle surface slope (small values of topographic gradient), presence of unstable rocks and relatively short distance to San Andreas fault. It should be mentioned

that algorithm does not supply information to conclude which factor among these three is the most important for amplification to occur. These characteristic traits are valid simultaneously only in this combination.

Topographic parameters including in D-traits reveal a little bit unexpected trend. In accordance with their values amplification-prone sites characterize by a gentle slope of the surface. It seemed to be more naturally if amplified sites will be characterized by steep slopes of the surface. Perhaps, this is connected with location of grids containing strong-motion station records which form the *D* class of the learning set. Most of them are located within flat areas surrounding San Francisco Bay. On the other hand, it is very probably that in the San Francisco region, for amplification of ground motions, site soil condition is more significant a factor than that of topography.

It is interesting that "short" distance to San Andreas fault turned out to be an important feature in identification of amplification-prone sites. As seen in Figure 2, most such sites are located rather far away from the source of the Loma Prieta earthquake.

It is necessary to emphasize that D-traits do not contain the parameters, such as AZ (azimuth), Dep (distance to epicenter) and Drup (distance to rupture zone), connected with position of amplification-prone sites relative to the epicenter of the Loma Prieta earthquake. By this, it is meant that a given D-trait might be applicable to the identification of amplification-prone sites in other regions affected by earthquakes as large as LPE.

The application of D traits to classification of control elements, not included in the learning set, has been shown to be reliable.

It should be mentioned herein that, probably, because of a rather large size of elements considered (5km by 5km), too generalized characterization of amplification-prone sites has been identified. It is observed that, very often, amplification can occur very locally within a small area, within a broad region that does not amplify ground motions. That is why the size of investigated elements should be carefully optimized in future studies.

Distribution of recognized amplification-prone elements over the San Francisco Peninsula demonstrates the rationality of the results. In Figure 14, the locations of 31 amplification-prone elements are shown. It is seen that these elements are mainly

concentrated in the northern part of the Peninsula and along the south-eastern shore of the San Francisco Bay. According to Hensolt and Brabb (1990), these areas are covered by a thick stratum of soft sediments overlying relatively consolidated bedrock. A number of protruded dome-shaped structures (subsurface topography) observed on the bedrock-surface under soft sediments may considerably complicate seismic wave propagation.

Elements 45,56,65,74 and 75 form a narrow strip extending in NW-SE direction along the junction of the Santa Cruz Mountains and Santa Clara basin. This boundary corresponds to fault tracing parallel to the San Andreas Fault (Wagner *et al.* , 1990). It is likely that during a large such as LPE, some faults in the vicinity of San Andreas fault may have been influenced; thus, causing the alterations of on strong motions.

Elements 24, 78, and 122 are isolated elements, on the Pacific Coast, that indicate amplification. Unlike the surrounding areas, these elements are characterized by relatively large areas of soft deposits.

Generally, it would be interesting to find some evidences to verify whether amplification took place during the Loma Prieta earthquake in all recognized elements.

In summary, we can conclude, first of all, that application of pattern recognition method to estimate strong ground motions gave us quite satisfactory results. As a result, particular set of site-conditions that possibly cause amplification of ground motions are defined. Amplification-prone sites within the San Francisco Peninsula are recognized.

This study should be considered as a first attempt to test PRM using strong motion data. To improve the results, in the future studies, it is necessary that: (a) the entire region affected by the Loma Prieta earthquake should be considered. This would improve the learning material and therefore the reliability of characteristic traits during the recognition process; (b) this decision rule be applied to another earthquake to verify the reasonability of decisions and assumption made in this study for identification of amplification-prone sites; (c) the optimal natural size of elements should be determined and more adequate list of topographic and geological parameters for their characterization be identified; (d) this approach is tested on other regions and the characteristic traits of amplification-prone sites are evaluated.

REFERENCES

- Aki, K., and Richards, P. G., 1980, **Quantitative Seismology: Theory and Methods**, Freeman and Co.
- Bhatia, S. C., Chetty, T. R. K., Filimonov, M., Gorshkov, A., Rantsman, E., and Rao, M. N., 1992, Identification of potential areas for the occurrence of strong earthquakes in Himalayan arc region, *Proc. Indian Acad. Sci. (Earth Planet. Sci)*, 1,4, pp. 369–385.
- Boore, D.M., 1987, The prediction of strong ground motion. *in* Strong Ground Motion Seismology (edited by M.Erdik and M.Toksoz), D.Reidel Publishing Company, pp. 109-142.
- Borcherdt, R. and Gibbs, J., 1976, Effects of local geological conditions in the San Francisco Bay region on ground motions and the intensities of 1906 earthquake, *Bull. Seism. Soc. Am.*, 66, pp. 467–500.
- Çelebi, M., 1987, Topographical and geological amplifications determined from strong-motion and aftershock records of the March 1985 Chile earthquake, *Bull. Seismol. Soc. Am.*, 77 (4), pp. 1147–1167.
- Çelebi, M., 1991, Topographical and geological amplification: case studies and engineering implications, *Structural Safety*, 10, pp. 199–217, Elsevier.
- Davis, L. L., and West, L. R., 1983, Observed effects of topography on ground motion *Bull. Seismol. Soc. Am.*, 63, pp. 283–298.
- EERI, 1990, Loma Prieta earthquake reconnaissance report, 90–06 (supplement to Volume 6), Earthquake Engineering Research Institute. El Cerrito, California, pp. 25–80.
- Geli, L., Bard, P. Y., and Jullien, B., 1988, The effect of topography on earthquake ground motion: a review and new results, *Bull. Seismol. Soc. Am.*, 78 (1), pp. 42–63.
- Gelfand, I. M., Guberman, Sh. A., Izvekova, M., Keilis–Borok, V., and Rantsman, E., 1972, Criteria of higher seismicity, *Doklady Akademii Nauk SSSR*, 202, 6, pp. 1317–1320.

- Gelfand, I. M., Guberman, Sh. A., Keilis-Borok, V., Knopoff L., Press, F., Rantsman E., Rotwain I., and Sadovsky A., 1976, Pattern recognition applied to earthquake epicenters in California, *Phys. Earth Planet. Int.*, 11, pp. 227-283.
- Gvishiani, A. D., Gorshkov, A. I., Rantsman E., Cisternas A., and Soloviev, A. A., 1988, **Identification of earthquake prone areas in regions of moderate seismicity**, Moscow Nauka, 175 pages (*in Russian*).
- Hall, T., *Map titled: The Effect of Soil Type on Earthquake Risk, date of publication not indicated*, Point Reyes National Seashore Association.
- Hanks, T. C. and Brady G., 1991, The Loma Prieta earthquake, ground motion and damage in Oakland, Treasure Island and San Francisco. *Bull. Seism. Soc. Am.* Vol. 81, N5, 2019–2047.
- Hensolt, W. and Brabb, E., 1990, Map showing elevation of bedrock and implications for design of engineered structures to withstand earthquake shaking in San Mateo County, California. USGS, Open-File Report No: 90-496.
- Holzer, T. L. and O'Rourke, T. D., 1990, Summary and conclusions in effects of the Loma Prieta earthquake on the Marina District, San Francisco, California. U.S. Geol. Survey Open-File Rept. 90-253, 1-6.
- Hough, S. E., Friberg, P. A., Busby, R., Field, E. F., Jacob, K. H., and Borchardt, R. D., 1990, Sediment-induced amplification and the collapse of the Nimitz freeway, *Nature*, 334, pp. 853–855.
- Maley, R., Acosta, A., Ellis, F., et.al., 1989, Strong-motion records from the Northern California (Loma Prieta) Earthquake of October 17, 1989. U.S. Geological Survey Open-File Report 89-568, 84p.
- Shakal, A., Huang, M., Reichle, M., et al., 1989, CSMIP strong-motion records from the Santa Cruz Mountains (Loma Prieta) California earthquake of October 17, 1989. Report No OSMS 89-06 California Strong Motion Instrumentation Program, 196p.

Shiga, T. A., Shibata, A., Shibuya, J., and Minami, R., 1979, Effects of irregular geophysical features on seismic ground motions, in Architectural Reports of Tohoku University, Department of Architecture, Tohoku Univ., Sendai, Japan.

USGS Staff, 1989, Lessons learned from the Loma Prieta, California, earthquake of October 17, 1989, U.S. Geological Survey Circular 1045, 48.

USGS Staff, 1990), The Loma Prieta, California, earthquake: an anticipated event. *Science* 247, 286–293.

Wagner, D. L., Bortugno, E. J., and McJunkin, R. D., (*compilers*), 1990, Geologic map of the San Francisco-San Jose Quadrangle, 1:250000.

Table 1. Parameters Used for the Description of Elements and Thresholds for Their Discretization.

#	Name of parameter	Thresholds of discretization and binary representation of parameter						
I. Topographical parameters:								
1	Maximum elevation within the square, (Hmax), m	<table border="1"> <tr> <td>'11'</td> <td>'01'</td> <td>'00'</td> </tr> <tr> <td>105.5</td> <td>259.0</td> <td></td> </tr> </table>	'11'	'01'	'00'	105.5	259.0	
'11'	'01'	'00'						
105.5	259.0							
2	Minimum elevation within the square, (Hmin), m	<table border="1"> <tr> <td>'11'</td> <td>'01'</td> <td>'00'</td> </tr> <tr> <td>0.5</td> <td>53.5</td> <td></td> </tr> </table>	'11'	'01'	'00'	0.5	53.5	
'11'	'01'	'00'						
0.5	53.5							
3	Distance between points of maximum and minimum elevations, (L), m							
4	Difference between maximum and minimum elevations (ΔH), m	<table border="1"> <tr> <td>'11'</td> <td>'01'</td> <td>'00'</td> </tr> <tr> <td>118.5</td> <td>247.5</td> <td></td> </tr> </table>	'11'	'01'	'00'	118.5	247.5	
'11'	'01'	'00'						
118.5	247.5							
5	Gradient ($\Delta H/L$)	<table border="1"> <tr> <td>'11'</td> <td>'01'</td> <td>'00'</td> </tr> <tr> <td>0.029</td> <td>0.059</td> <td></td> </tr> </table>	'11'	'01'	'00'	0.029	0.059	
'11'	'01'	'00'						
0.029	0.059							
6	Topography (landforms) within the square (Topog):							
	1 - hills	'1000'						
	2 - flat area	'0100'						
	3 - slope	'0010'						
	4 - ridge	'0001'						
	5 - ridge/slope	'0001'						
	6 - slope/flat	'0001'						
II. Geological parameters:								
7	Soil types (Soil):							
	1 - stable rock	'100'						
	2 - unstable rock	'010'						
	3 - unconsolidated soil	'001'						
	4 - mud and fill	'001'						
III. Other parameters:								
8	Distance to the epicenter from the center of square, (Dep), km							
9	Distance to San Andreas fault from the center of square, (DSF), km	<table border="1"> <tr> <td>'11'</td> <td>'01'</td> <td>'00'</td> </tr> <tr> <td>4.8</td> <td>11.4</td> <td></td> </tr> </table>	'11'	'01'	'00'	4.8	11.4	
'11'	'01'	'00'						
4.8	11.4							
10	Azimuth from the epicenter to the center of square, (Az)	<table border="1"> <tr> <td>'11'</td> <td>'00'</td> </tr> <tr> <td>327.5</td> <td></td> </tr> </table>	'11'	'00'	327.5			
'11'	'00'							
327.5								
11	Distance to the rupture zone from the center of square, (Drup), km							

Table 2. Seismic Stations and Peak Ground Accelerations Recorded During the Loma Prieta Earthquake.

USGS STATIONS FOR Loma Prieta

Name	Epicentral Distance (km)	PGA (g)	Within the Element #
1. S.F. State University	93	0.14	6
2. S.F. Golden Gate Bridge	100	0.24	1
3. S.F. 1295 Shafter	89	0.11	8
4. Redwood City	63	0.28	23
5. Foster City	66	0.12	23
6. Crystal Springs Reserv.	62	0.12	33
7. Stanford, SLAC	51	0.29	44
8. Menlo Park VA	54	0.27	36
9. Palo Alto VA	47	0.38	45
10. Sunnyvale	43	0.22	47
11. San Jose Interchange	34	0.18	58

CSMIP STATIONS FOR L-P EQ, 1989

Name	Epicentral Distance (km)	PGA (g)	Within the Element #
1. S.F. Presidio	98	0.21	3
2. S.F. Telegraph Hill	97	0.08	2
3. S.F. Pacific Heights	97	0.08	4
4. S.F. Rincon Hill	95	0.09	5
5. S.F. Cliff House	99	0.11	3
6. S.F. Diamond Heights	92	0.12	7
7. S.F. Sierra Point	84	0.11	11
8. S.F. Sierra Pt. Overpass	84	0.09	11
9. S.F. Internat. Airport	79	0.33	14
10. Foster City	63	0.29	23
11. Lower Crystal	69	0.09	21
12. Upper Crystal (58373)	63	0.10	33
13. Belmont	65	0.11	27
14. Upper Crystal (58378)	63	0.16	27
15. Redwood City	57	0.09	34
16. Woodside	55	0.08	43
17. Palo Alto	50	0.21	36
18. Agnew	40	0.17	48
19. Milpitas	43	0.14	49
20. Saratoga (58235)	27	0.33	74
21. Saratoga (58065)	27	0.53	74
22. Lexington Dam	19	0.45	85
23. San Jose (57 563)	21	0.28	88
24. San Jose (57 562)	21	0.20	88
25. Corralitos	7	0.64	126
26. Santa Cruz	16	0.47	129
27. Capitola	9	0.60	130

Table 3. Characteristic D-traits and N-traits of Elements Selected by CORA-3 Algorithm.

Parameters							
#	Hmin	Hmax	ΔH	DSF	Gradient	Topog	Soil
D-traits							
1					<0.059	not slope	not stable rock
2		>105.5				whether hills, or flat area, or slope	
3		>105.5			<0.059		
4				<11.4		not ridge not ridge/slope not slope/flat	
5		<247.5	>4.8			not slope	
N-traits							
1	>0.5					not slope	not unstable rock
2	>0.5					not hills	not unstable rock
3					>0.029	not hills	
4	>0.5				>0.029		

Table 4. Values of Parameters of Elements.

# and name :	1 : Hmax :	2 : Hmin :	3 : L :	4 : ΔH :	5 : $\Delta H/L$:	6 : Topog :
1. sf1:	113.00:	-37.00:	3200.00:	150.00:	0.05:	1.00:
2. sf2:	98.00:	-37.00:	3100.00:	135.00:	0.04:	1.00:
3. sf3:	203.00:	-9.00:	3700.00:	212.00:	0.06:	1.00:
4. sf4:	274.00:	18.00:	4700.00:	256.00:	0.05:	1.00:
5. sf5:	91.00:	-15.00:	3100.00:	106.00:	0.03:	2.00:
6. sf6:	152.00:	-12.00:	4400.00:	164.00:	0.04:	1.00:
7. sf7:	274.00:	15.00:	4400.00:	259.00:	0.06:	1.00:
8. sf8:	122.00:	-9.00:	2400.00:	131.00:	0.05:	1.00:
9. sf9:	213.00:	-15.00:	1900.00:	228.00:	0.12:	1.00:
10. sf10:	396.00:	30.00:	2700.00:	366.00:	0.14:	1.00:
11. sf11:	244.00:	-7.00:	3100.00:	251.00:	0.08:	3.00:
12. sf12:	152.00:	-14.00:	3400.00:	166.00:	0.05:	2.00:
13. sf13:	244.00:	6.00:	6200.00:	238.00:	0.04:	2.00:
14. sf14:	6.00:	-13.00:	4600.00:	19.00:	0.00:	2.00:
15. sf15:	305.00:	0.00:	3100.00:	305.00:	0.10:	3.00:
16. sf16:	427.00:	122.00:	2700.00:	305.00:	0.11:	5.00:
17. sf17:	163.00:	-2.00:	6200.00:	165.00:	0.03:	2.00:
18. sf18:	11.00:	-12.00:	6400.00:	23.00:	0.00:	2.00:
19. sf19:	549.00:	0.00:	3000.00:	549.00:	0.18:	3.00:
20. sf20:	427.00:	211.00:	1600.00:	216.00:	0.14:	4.00:
21. sf21:	305.00:	61.00:	2700.00:	244.00:	0.09:	6.00:
22. sf22:	152.00:	0.00:	5700.00:	152.00:	0.03:	2.00:
23. sf23:	9.00:	0.00:	6200.00:	9.00:	0.00:	2.00:
24. sf24:	244.00:	-34.00:	6500.00:	278.00:	0.04:	2.00:
25. sf25:	488.00:	46.00:	4100.00:	442.00:	0.11:	3.00:
26. sf26:	305.00:	110.00:	1700.00:	195.00:	0.12:	4.00:
27. sf27:	305.00:	122.00:	5000.00:	183.00:	0.04:	3.00:
28. sf28:	61.00:	3.00:	4900.00:	58.00:	0.01:	2.00:
29. sf29:	5.00:	1.00:	4200.00:	4.00:	0.00:	2.00:
30. sf30:	3.00:	-12.00:	5000.00:	15.00:	0.00:	2.00:
31. sf31:	244.00:	61.00:	1700.00:	183.00:	0.11:	6.00:
32. sf32:	549.00:	107.00:	4500.00:	442.00:	0.10:	3.00:
33. sf33:	610.00:	122.00:	3500.00:	488.00:	0.14:	4.00:
34. sf34:	183.00:	24.00:	5200.00:	159.00:	0.03:	2.00:
35. sf35:	55.00:	6.00:	5500.00:	49.00:	0.01:	2.00:
36. sf36:	30.00:	0.00:	5000.00:	30.00:	0.01:	2.00:
37. sf37:	2.00:	-1.00:	5600.00:	3.00:	0.00:	2.00:
38. sf38:	1.00:	-3.00:	5700.00:	4.00:	0.00:	2.00:
39. sf39:	1.00:	1.00:	5600.00:	0.00:	0.00:	2.00:
40. sf40:	215.00:	-18.00:	3100.00:	233.00:	0.08:	3.00:
41. sf41:	641.00:	122.00:	5700.00:	519.00:	0.09:	3.00:
42. sf42:	706.00:	305.00:	3000.00:	401.00:	0.13:	4.00:
43. sf43:	610.00:	122.00:	3900.00:	488.00:	0.12:	6.00:
44. sf44:	183.00:	91.00:	3000.00:	92.00:	0.03:	2.00:
45. sf45:	113.00:	9.00:	4000.00:	104.00:	0.03:	2.00:
46. sf46:	22.00:	1.00:	4400.00:	21.00:	0.00:	2.00:
47. sf47:	27.00:	1.00:	6000.00:	26.00:	0.00:	2.00:
48. sf48:	9.00:	1.00:	4500.00:	8.00:	0.00:	2.00:
49. sf49:	12.00:	3.00:	4700.00:	9.00:	0.00:	2.00:
50. sf50:	305.00:	-3.00:	4700.00:	308.00:	0.07:	3.00:
51. sf51:	610.00:	122.00:	4000.00:	488.00:	0.12:	3.00:
52. sf52:	671.00:	152.00:	4000.00:	519.00:	0.13:	3.00:
53. sf53:	610.00:	183.00:	3100.00:	427.00:	0.14:	3.00:

54. sf54:	366.00:	76.00:	3900.00:	290.00:	0.07:	3.00:
55. sf55:	122.00:	67.00:	5900.00:	55.00:	0.01:	2.00:
56. sf56:	61.00:	27.00:	4600.00:	34.00:	0.01:	2.00:
57. sf57:	30.00:	9.00:	4500.00:	21.00:	0.00:	2.00:
58. sf58:	27.00:	11.00:	4000.00:	16.00:	0.00:	2.00:
59. sf59:	256.00:	0.00:	5000.00:	256.00:	0.05:	3.00:
60. sf60:	366.00:	46.00:	3100.00:	320.00:	0.10:	3.00:
61. sf61:	671.00:	152.00:	3900.00:	519.00:	0.13:	3.00:
62. sf62:	784.00:	335.00:	2500.00:	449.00:	0.18:	4.00:
63. sf63:	792.00:	488.00:	1500.00:	304.00:	0.20:	4.00:
64. sf64:	549.00:	152.00:	3100.00:	397.00:	0.13:	3.00:
65. sf65:	104.00:	61.00:	4400.00:	43.00:	0.01:	2.00:
66. sf66:	67.00:	30.00:	5900.00:	37.00:	0.01:	2.00:
67. sf67:	55.00:	27.00:	6700.00:	28.00:	0.00:	2.00:
68. sf68:	305.00:	9.00:	4700.00:	296.00:	0.06:	3.00:
69. sf69:	500.00:	46.00:	2100.00:	454.00:	0.22:	4.00:
70. sf70:	550.00:	107.00:	2000.00:	443.00:	0.22:	3.00:
71. sf71:	485.00:	168.00:	4100.00:	317.00:	0.08:	3.00:
72. sf72:	815.00:	366.00:	2500.00:	449.00:	0.18:	4.00:
73. sf73:	853.00:	244.00:	4400.00:	609.00:	0.14:	3.00:
74. sf74:	244.00:	91.00:	5900.00:	153.00:	0.03:	2.00:
75. sf75:	94.00:	58.00:	5100.00:	36.00:	0.01:	2.00:
76. sf76:	66.00:	52.00:	4000.00:	14.00:	0.00:	2.00:
77. sf77:	67.00:	49.00:	2500.00:	18.00:	0.01:	2.00:
78. sf78:	183.00:	12.00:	5700.00:	171.00:	0.03:	3.00:
79. sf79:	366.00:	46.00:	1500.00:	320.00:	0.21:	4.00:
80. sf80:	671.00:	305.00:	1400.00:	366.00:	0.26:	4.00:
81. sf81:	719.00:	152.00:	2900.00:	567.00:	0.20:	4.00:
82. sf82:	624.00:	305.00:	1500.00:	319.00:	0.21:	3.00:
83. sf83:	914.00:	305.00:	2700.00:	609.00:	0.23:	4.00:
84. sf84:	732.00:	183.00:	3400.00:	549.00:	0.16:	3.00:
85. sf85:	610.00:	94.00:	4900.00:	516.00:	0.10:	3.00:
86. sf86:	732.00:	76.00:	5600.00:	656.00:	0.12:	3.00:
87. sf87:	183.00:	61.00:	4200.00:	122.00:	0.03:	1.00:
88. sf88:	313.00:	46.00:	3100.00:	267.00:	0.09:	1.00:
89. sf89:	185.00:	-37.00:	4600.00:	222.00:	0.05:	3.00:
90. sf90:	427.00:	46.00:	4600.00:	381.00:	0.08:	3.00:
91. sf91:	549.00:	61.00:	2600.00:	488.00:	0.19:	3.00:
92. sf92:	610.00:	274.00:	4400.00:	336.00:	0.08:	3.00:
93. sf93:	366.00:	183.00:	1200.00:	183.00:	0.15:	4.00:
94. sf94:	674.00:	274.00:	1500.00:	400.00:	0.27:	4.00:
95. sf95:	688.00:	335.00:	2400.00:	353.00:	0.15:	4.00:
96. sf96:	792.00:	197.00:	2700.00:	595.00:	0.22:	4.00:
97. sf97:	1063.00:	187.00:	4600.00:	876.00:	0.19:	4.00:
98. sf98:	728.00:	187.00:	3200.00:	541.00:	0.17:	3.00:
99. sf99:	560.00:	120.00:	4400.00:	440.00:	0.10:	3.00:
100. sf100:	427.00:	61.00:	2700.00:	366.00:	0.14:	6.00:
101. sf101:	366.00:	61.00:	1200.00:	305.00:	0.25:	3.00:
102. sf102:	758.00:	427.00:	4100.00:	331.00:	0.08:	3.00:
103. sf103:	802.00:	488.00:	2400.00:	314.00:	0.13:	4.00:
104. sf104:	366.00:	176.00:	1500.00:	190.00:	0.13:	3.00:
105. sf105:	511.00:	176.00:	2600.00:	335.00:	0.13:	3.00:
106. sf106:	610.00:	305.00:	2700.00:	305.00:	0.11:	4.00:
107. sf107:	1003.00:	610.00:	3200.00:	393.00:	0.12:	3.00:
108. sf108:	1155.00:	549.00:	4400.00:	606.00:	0.14:	4.00:
109. sf109:	975.00:	274.00:	3200.00:	701.00:	0.22:	3.00:
110. sf110:	366.00:	-27.00:	5900.00:	393.00:	0.07:	3.00:
111. sf111:	581.00:	55.00:	4500.00:	526.00:	0.12:	3.00:
112. sf112:	792.00:	366.00:	4400.00:	426.00:	0.10:	4.00:
113. sf113:	488.00:	176.00:	4600.00:	312.00:	0.07:	3.00:

114.sf114:	444.00:	152.00:	3900.00:	292.00:	0.08:	3.00:
115.sf115:	364.00:	107.00:	4600.00:	257.00:	0.06:	3.00:
116.sf116:	671.00:	122.00:	4600.00:	549.00:	0.12:	3.00:
117.sf117:	905.00:	488.00:	1400.00:	417.00:	0.30:	4.00:
118.sf118:	853.00:	366.00:	2400.00:	487.00:	0.20:	4.00:
119.sf119:	366.00:	-18.00:	5000.00:	384.00:	0.08:	3.00:
120.sf120:	549.00:	122.00:	5200.00:	427.00:	0.08:	3.00:
121.sf121:	323.00:	91.00:	4400.00:	232.00:	0.05:	3.00:
122.sf122:	244.00:	122.00:	4500.00:	122.00:	0.03:	1.00:
123.sf123:	244.00:	61.00:	4700.00:	183.00:	0.04:	3.00:
124.sf124:	427.00:	67.00:	4100.00:	360.00:	0.09:	4.00:
125.sf125:	671.00:	122.00:	4900.00:	549.00:	0.11:	3.00:
126.sf126:	732.00:	152.00:	5400.00:	580.00:	0.11:	3.00:
127.sf127:	305.00:	-27.00:	5700.00:	332.00:	0.06:	3.00:
128.sf128:	305.00:	61.00:	4000.00:	244.00:	0.06:	3.00:
129.sf129:	244.00:	46.00:	4100.00:	198.00:	0.05:	3.00:
130.sf130:	183.00:	18.00:	4600.00:	165.00:	0.04:	3.00:
131.sf131:	244.00:	-6.00:	4100.00:	250.00:	0.06:	3.00:
132.sf132:	366.00:	46.00:	5700.00:	320.00:	0.06:	3.00:
133.sf133:	396.00:	61.00:	5900.00:	335.00:	0.06:	3.00:

Continued.

Table 4. Continuation.

# and name	7 Soil	8 Dep	9 DSF	10 Az	11 Drup
1. sf1:	3.00:	100.60:	8.60:	325.00:	86.00:
2. sf2:	3.00:	98.10:	12.50:	328.00:	84.00:
3. sf3:	1.00:	96.20:	5.50:	327.00:	82.50:
4. sf4:	1.00:	93.70:	10.00:	330.00:	80.00:
5. sf5:	3.00:	91.20:	15.00:	332.00:	76.90:
6. sf6:	3.00:	92.50:	3.10:	325.00:	78.10:
7. sf7:	1.00:	89.40:	7.70:	327.00:	75.50:
8. sf8:	4.00:	86.90:	12.10:	330.00:	73.10:
9. sf9:	3.00:	88.10:	1.10:	323.00:	73.70:
10. sf10:	1.00:	85.60:	5.00:	325.00:	71.20:
11. sf11:	4.00:	82.90:	9.20:	329.00:	68.70:
12. sf12:	1.00:	84.40:	1.90:	321.00:	70.60:
13. sf13:	3.00:	81.20:	2.20:	325.00:	67.10:
14. sf14:	4.00:	78.50:	6.20:	328.00:	64.40:
15. sf15:	2.00:	80.60:	4.90:	320.00:	66.60:
16. sf16:	2.00:	76.90:	0.90:	322.00:	63.10:
17. sf17:	3.00:	74.40:	3.20:	326.00:	60.20:
18. sf18:	4.00:	71.90:	7.50:	329.00:	57.60:
19. sf19:	1.00:	76.90:	8.00:	317.00:	66.70:
20. sf20:	1.00:	73.50:	3.70:	320.00:	59.40:
21. sf21:	1.00:	69.00:	0.20:	323.00:	56.20:
22. sf22:	3.00:	67.50:	4.50:	327.00:	53.10:
23. sf23:	4.00:	64.60:	8.50:	331.00:	50.20:
24. sf24:	1.00:	73.40:	10.90:	313.00:	59.90:
25. sf25:	1.00:	69.60:	6.60:	316.00:	55.90:
26. sf26:	1.00:	66.20:	2.50:	319.00:	52.40:
27. sf27:	1.00:	63.20:	1.50:	323.00:	49.00:
28. sf28:	2.00:	60.20:	5.60:	327.00:	46.00:
29. sf29:	4.00:	57.50:	9.70:	332.00:	43.40:
30. sf30:	4.00:	55.40:	13.70:	336.00:	41.20:
31. sf31:	2.00:	66.00:	9.60:	314.00:	52.50:
32. sf32:	1.00:	62.50:	5.60:	317.00:	48.70:
33. sf33:	1.00:	59.10:	1.50:	321.00:	45.10:
34. sf34:	1.00:	56.00:	2.70:	325.00:	42.00:
35. sf35:	3.00:	53.40:	6.60:	329.00:	39.00:
36. sf36:	3.00:	50.90:	10.70:	334.00:	36.50:
37. sf37:	4.00:	48.90:	15.00:	340.00:	34.60:
38. sf38:	4.00:	47.20:	19.20:	346.00:	33.40:
39. sf39:	4.00:	46.20:	22.70:	352.00:	32.50:
40. sf40:	3.00:	62.50:	12.70:	311.00:	49.40:
41. sf41:	2.00:	58.70:	8.40:	314.00:	45.40:
42. sf42:	1.00:	55.20:	4.50:	318.00:	41.50:
43. sf43:	1.00:	51.90:	0.40:	322.00:	38.00:
44. sf44:	1.00:	49.00:	3.50:	327.00:	35.00:
45. sf45:	1.00:	46.20:	7.70:	332.00:	32.10:
46. sf46:	3.00:	44.00:	11.90:	338.00:	29.70:
47. sf47:	3.00:	42.40:	15.60:	344.00:	28.20:
48. sf48:	3.00:	41.20:	19.00:	351.00:	27.50:
49. sf49:	3.00:	40.60:	22.60:	358.00:	28.10:
50. sf50:	2.00:	55.40:	11.50:	310.00:	42.40:
51. sf51:	2.00:	51.60:	7.50:	313.00:	38.20:
52. sf52:	2.00:	48.10:	3.50:	318.00:	34.40:
53. sf53:	2.00:	44.70:	0.60:	323.00:	30.90:
54. sf54:	1.00:	41.90:	4.90:	328.00:	27.70:

55. sf55:	3.00:	39.50:	8.40:	334.00:	25.20:
56. sf56:	3.00:	37.50:	11.90:	341.00:	23.40:
57. sf57:	3.00:	36.20:	15.50:	349.00:	22.90:
58. sf58:	3.00:	35.60:	19.20:	357.00:	23.10:
59. sf59:	2.00:	52.20:	14.60:	306.00:	39.60:
60. sf60:	2.00:	48.40:	10.50:	310.00:	35.20:
61. sf61:	2.00:	44.40:	6.40:	314.00:	31.00:
62. sf62:	2.00:	40.90:	2.40:	319.00:	27.10:
63. sf63:	1.00:	37.70:	1.10:	324.00:	23.60:
64. sf64:	2.00:	35.00:	4.70:	331.00:	20.90:
65. sf65:	3.00:	32.90:	8.20:	338.00:	18.70:
66. sf66:	3.00:	31.20:	12.00:	348.00:	17.50:
67. sf67:	3.00:	30.60:	15.50:	357.00:	18.10:
68. sf68:	3.00:	49.60:	17.50:	301.00:	37.50:
69. sf69:	2.00:	45.20:	13.40:	304.00:	33.00:
70. sf70:	1.00:	40.90:	9.50:	308.00:	28.40:
71. sf71:	2.00:	37.10:	6.00:	313.00:	24.00:
72. sf72:	2.00:	33.50:	2.50:	319.00:	19.90:
73. sf73:	1.00:	30.60:	1.10:	326.00:	16.50:
74. sf74:	2.00:	28.10:	4.90:	335.00:	14.00:
75. sf75:	3.00:	26.50:	8.40:	345.00:	12.70:
76. sf76:	3.00:	25.60:	12.00:	356.00:	13.40:
77. sf77:	3.00:	25.60:	15.40:	7.00:	15.60:
78. sf78:	2.00:	46.90:	20.50:	295.00:	36.20:
79. sf79:	2.00:	42.50:	16.60:	298.00:	31.20:
80. sf80:	2.00:	38.20:	13.10:	302.00:	26.40:
81. sf81:	2.00:	34.00:	9.60:	307.00:	21.60:
82. sf82:	2.00:	30.00:	6.00:	313.00:	17.00:
83. sf83:	2.00:	26.60:	2.50:	320.00:	12.90:
84. sf84:	2.00:	23.70:	1.20:	330.00:	9.50:
85. sf85:	2.00:	21.60:	4.70:	341.00:	7.70:
86. sf86:	2.00:	20.50:	8.20:	355.00:	8.50:
87. sf87:	3.00:	20.60:	11.90:	8.00:	11.90:
88. sf88:	3.00:	22.10:	15.20:	21.00:	15.00:
89. sf89:	3.00:	45.10:	23.70:	290.00:	35.10:
90. sf90:	2.00:	40.40:	20.20:	292.00:	30.00:
91. sf91:	1.00:	35.70:	16.70:	295.00:	25.00:
92. sf92:	1.00:	31.20:	13.20:	299.00:	20.00:
93. sf93:	1.00:	27.10:	9.60:	304.00:	15.20:
94. sf94:	2.00:	22.90:	6.00:	311.00:	10.20:
95. sf95:	1.00:	19.40:	2.50:	322.00:	5.60:
96. sf96:	2.00:	16.70:	1.10:	336.00:	2.50:
97. sf97:	2.00:	15.50:	4.70:	353.00:	4.70:
98. sf98:	2.00:	15.60:	8.00:	12.00:	7.50:
99. sf99:	2.00:	17.40:	11.00:	28.00:	11.00:
100. sf100:	3.00:	38.70:	24.00:	285.00:	30.00:
101. sf101:	2.00:	33.70:	20.40:	287.00:	24.70:
102. sf102:	1.00:	29.20:	16.70:	291.00:	19.70:
103. sf103:	1.00:	24.50:	13.20:	295.00:	14.70:
104. sf104:	2.00:	19.90:	9.60:	300.00:	9.50:
105. sf105:	1.00:	15.70:	6.00:	311.00:	4.50:
106. sf106:	2.00:	12.40:	2.50:	326.00:	0.00:
107. sf107:	2.00:	10.40:	0.90:	350.00:	0.60:
108. sf108:	1.00:	10.90:	3.90:	18.00:	3.90:
109. sf109:	2.00:	13.10:	6.90:	40.00:	6.90:
110. sf110:	2.00:	32.70:	23.90:	279.00:	25.50:
111. sf111:	1.00:	27.70:	20.40:	281.00:	20.40:
112. sf112:	1.00:	22.70:	16.70:	283.00:	15.40:
113. sf113:	2.00:	17.90:	13.40:	287.00:	10.50:
114. sf114:	2.00:	13.10:	9.60:	293.00:	5.60:

115.sf115:	2.00:	8.60:	6.20:	306.00:	0.60:
116.sf116:	2.00:	5.50:	2.60:	341.00:	0.00:
117.sf117:	2.00:	6.00:	0.00:	33.00:	0.00:
118.sf118:	1.00:	9.70:	2.90:	58.00:	3.00:
119.sf119:	2.00:	27.40:	24.10:	270.00:	21.70:
120.sf120:	1.00:	21.40:	20.40:	270.00:	16.90:
121.sf121:	1.00:	17.00:	16.70:	270.00:	12.20:
122.sf122:	2.00:	12.00:	13.40:	270.00:	7.90:
123.sf123:	2.00:	6.90:	10.40:	270.00:	3.90:
124.sf124:	2.00:	1.90:	7.20:	270.00:	0.60:
125.sf125:	1.00:	3.10:	4.10:	90.00:	0.00:
126.sf126:	1.00:	8.20:	0.90:	90.00:	0.00:
127.sf127:	2.00:	23.00:	24.20:	257.00:	19.20:
128.sf128:	2.00:	17.70:	20.60:	254.00:	14.90:
129.sf129:	1.00:	13.00:	17.60:	248.00:	11.20:
130.sf130:	2.00:	8.40:	14.40:	235.00:	8.00:
131.sf131:	2.00:	5.20:	11.20:	202.00:	5.00:
132.sf132:	2.00:	5.90:	8.10:	148.00:	2.10:
133.sf133:	2.00:	9.70:	4.40:	121.00:	0.00:
-----:-----:-----:-----:-----:-----:					

Table 5. Control Elements: Recorded Peak Ground Accelerations (PGA), Epicentral Distance (DEP) and Calculated Characteristic PGA_1 .

# and name of element	PGA	DEP	PGA1
sf134	0.29	95	27.55
sf135	0.26	92	23.92
sf136	0.08	93	7.44
sf137	0.18	71	12.78
sf138	0.13	55	7.15
sf139	0.13	37	4.81
sf140	0.08	27	2.16

Table 6. Parameters of Control Elements.

# and name of element:	1 : Hmin	2 : Hmax	3 : ΔH	4 : DSF	5 : $\Delta H/L$	6 : Topog	7 : Soil
1.sf134:	-7.90:	6.00:	-1.90:	20.75:	0.00:	flat area:	mud and fil
2.sf135:	0.00:	48.80:	48.80:	25.50:	0.01:	flat area:	unconsolid.soil:
3.sf136:	12.20:	365.80:	353.60:	30.10:	0.09:	hills	unconsolid.soil:
4.sf137:	15.20:	182.90:	167.70:	30.00:	0.04:	hills	unconsolid.soil:
5.sf138:	4.80:	45.70:	40.90:	24.75:	0.00:	flat area:	unconsolid.soil:
6.sf139:	518.10:	901.00:	383.00:	31.50:	0.16:	ridge	unstable bedrock:
7.sf140:	190.50:	419.70:	229.20:	20.75:	0.15:	ridge	stable bedrock:

Table 7. Result of Classification of Control Elements.

# and name of element	number of D-traits (Nd)	number of N-traits (Nn)
sf134	2	0
sf135	1	0
sf136	1	2
sf137	3	2
sf138	1	2
sf139	0	0
sf140	1	2

Table 8. Binary Representation of Parameters Forming Decision Rule.

		A:	z:	i:	n:	a:	x:	l:	ΔH :	S:	ΔH :	F:	L:	D:	Topog	Soil
1.	sf1	1:1	1:0	1:1:0	1:0	1:0	1:1	0	0	0:0	0	0	1:			
2.	sf2	0:1	1:1	1:1:0	1:0	0:0	1:1	0	0	0:0	0	0	1:			
3.	sf3	1:1	1:0	1:1:0	1:0	1:0	1:1	0	0	0:1	0	0:				
4.	sf4	0:0	1:0	0:0:0	0:0	1:0	1:1	0	0	0:1	0	0:				
5.	sf5	0:1	1:1	1:1:1	1:0	0:0	1:0	1	0	0:0	0	1:				
6.	sf6	1:1	1:0	1:1:0	1:1	1:0	1:1	0	0	0:0	0	1:				
7.	sf7	1:0	1:0	0:1:0	0:0	1:0	1:1	0	0	0:1	0	0:				
8.	sf8	0:1	1:0	1:1:0	1:0	0:0	1:1	0	0	0:0	0	1:				
9.	sf9	1:1	1:0	1:1:0	1:1	1:0	0:1	0	0	0:0	0	1:				
10.	sf10	1:0	1:0	0:1:0	0:0	1:0	0:1	0	0	0:1	0	0:				
11.	sf11	0:1	1:0	1:1:0	0:0	1:0	0:0	0	1	0:0	0	1:				
12.	sf12	1:1	1:0	1:1:0	1:1	1:0	1:0	1	0	0:1	0	0:				
13.	sf13	1:0	1:0	1:0:0	1:1	1:0	1:0	1	0	0:0	0	1:				
14.	sf14	0:1	1:1	1:0:1	1:0	1:1	1:0	1	0	0:0	0	1:				
15.	sf15	1:1	1:0	0:1:0	0:0	1:0	0:0	0	1	0:0	1	0:				
16.	sf16	1:0	0:0	0:1:0	0:1	1:0	0:0	0	0	1:0	1	0:				
17.	sf17	1:1	1:0	1:0:0	1:1	1:1	1:0	1	0	0:0	0	1:				
18.	sf18	0:1	1:1	1:0:1	1:0	1:1	1:0	1	0	0:0	0	1:				
19.	sf19	1:1	1:0	0:1:0	0:0	1:0	0:0	0	1	0:1	0	0:				
20.	sf20	1:0	0:0	0:1:0	1:1	1:0	0:0	0	0	1:1	0	0:				
21.	sf21	1:0	0:0	0:1:0	1:1	1:0	0:0	0	0	1:1	0	0:				
22.	sf22	1:1	1:0	1:0:0	1:1	1:1	1:0	1	0	0:0	0	1:				
23.	sf23	0:1	1:1	1:0:1	1:0	1:1	1:0	1	0	0:0	0	1:				
24.	sf24	1:1	1:0	1:0:0	0:0	1:0	1:0	1	0	0:1	0	0:				
25.	sf25	1:0	1:0	0:1:0	0:0	1:0	0:0	0	1	0:1	0	0:				
26.	sf26	1:0	0:0	0:1:0	1:1	1:0	0:0	0	0	1:1	0	0:				
27.	sf27	1:0	0:0	0:0:0	1:1	1:0	1:0	0	1	0:1	0	0:				
28.	sf28	1:0	1:1	1:0:1	1:0	1:1	1:0	1	0	0:0	1	0:				
29.	sf29	0:0	1:1	1:1:1	1:0	1:1	1:0	1	0	0:0	0	1:				
30.	sf30	0:1	1:1	1:0:1	1:0	0:1	1:0	1	0	0:0	0	1:				
31.	sf31	1:0	0:0	1:1:0	1:0	1:0	0:0	0	0	1:0	1	0:				
32.	sf32	1:0	0:0	0:0:0	0:0	1:0	0:0	0	1	0:1	0	0:				
33.	sf33	1:0	0:0	0:1:0	0:1	1:0	0:0	0	0	1:1	0	0:				
34.	sf34	1:0	1:0	1:0:0	1:1	1:0	1:0	1	0	0:1	0	0:				
35.	sf35	0:0	1:1	1:0:1	1:0	1:1	1:0	1	0	0:0	0	1:				
36.	sf36	0:1	1:1	1:0:1	1:0	1:1	1:0	1	0	0:0	0	1:				
37.	sf37	0:1	1:1	1:0:1	1:0	0:1	1:0	1	0	0:0	0	1:				
38.	sf38	0:1	1:1	1:0:1	1:0	0:1	1:0	1	0	0:0	0	1:				
39.	sf39	0:0	1:1	1:0:1	1:0	0:1	1:0	1	0	0:0	0	1:				
40.	sf40	1:1	1:0	1:1:0	1:0	0:0	0:0	0	1	0:0	0	1:				
41.	sf41	1:0	0:0	0:0:0	0:0	1:0	0:0	0	1	0:0	1	0:				
42.	sf42	1:0	0:0	0:1:0	0:1	1:0	0:0	0	0	1:1	0	0:				
43.	sf43	1:0	0:0	0:1:0	0:1	1:0	0:0	0	0	1:1	0	0:				
44.	sf44	1:0	0:0	1:1:1	1:1	1:1	1:0	1	0	0:1	0	0:				
45.	sf45	0:0	1:0	1:1:1	1:0	1:1	1:0	1	0	0:1	0	0:				
46.	sf46	0:0	1:1	1:1:1	1:0	0:1	1:0	1	0	0:0	0	1:				
47.	sf47	0:0	1:1	1:0:1	1:0	0:1	1:0	1	0	0:0	0	1:				
48.	sf48	0:0	1:1	1:0:1	1:0	0:1	1:0	1	0	0:0	0	1:				
49.	sf49	0:0	1:1	1:0:1	1:0	0:1	1:0	1	0	0:0	0	1:				

To be continued...

Table 8. Continuation.

50.	sf50	1:1	1:0	0:0:0	0:0	0:0	0:0	0	1	0:0	1	0:
51.	sf51	1:0	0:0	0:1:0	0:0	1:0	0:0	0	1	0:0	1	0:
52.	sf52	1:0	0:0	0:1:0	0:1	1:0	0:0	0	1	0:0	1	0:
53.	sf53	1:0	0:0	0:1:0	0:1	1:0	0:0	0	1	0:0	1	0:
54.	sf54	0:0	0:0	0:1:0	0:0	1:0	0:0	0	1	0:1	0	0:
55.	sf55	0:0	0:0	1:0:1	1:0	1:1	1:0	1	0	0:0	0	1:
56.	sf56	0:0	1:1	1:0:1	1:0	0:1	1:0	1	0	0:0	0	1:
57.	sf57	0:0	1:1	1:0:1	1:0	0:1	1:0	1	0	0:0	0	1:
58.	sf58	0:0	1:1	1:1:1	1:0	0:1	1:0	1	0	0:0	0	1:
59.	sf59	1:1	1:0	1:0:0	0:0	0:0	1:0	0	1	0:0	1	0:
60.	sf60	1:0	1:0	0:1:0	0:0	1:0	0:0	0	1	0:0	1	0:
61.	sf61	1:0	0:0	0:1:0	0:0	1:0	0:0	0	1	0:0	1	0:
62.	sf62	1:0	0:0	0:1:0	0:1	1:0	0:0	0	0	1:0	1	0:
63.	sf63	1:0	0:0	0:1:0	0:1	1:0	0:0	0	0	1:1	0	0:
64.	sf64	0:0	0:0	0:1:0	0:1	1:0	0:0	0	1	0:0	1	0:
65.	sf65	0:0	0:1	1:1:1	1:0	1:1	1:0	1	0	0:0	0	1:
66.	sf66	0:0	1:1	1:0:1	1:0	0:1	1:0	1	0	0:0	0	1:
67.	sf67	0:0	1:1	1:0:1	1:0	0:1	1:0	1	0	0:0	0	1:
68.	sf68	1:0	1:0	0:0:0	0:0	0:0	0:0	0	1	0:0	0	1:
69.	sf69	1:0	1:0	0:1:0	0:0	0:0	0:0	0	0	1:0	1	0:
70.	sf70	1:0	0:0	0:1:0	0:0	1:0	0:0	0	1	0:1	0	0:
71.	sf71	1:0	0:0	0:1:0	0:0	1:0	0:0	0	1	0:0	1	0:
72.	sf72	1:0	0:0	0:1:0	0:1	1:0	0:0	0	0	1:0	1	0:
73.	sf73	1:0	0:0	0:1:0	0:1	1:0	0:0	0	1	0:1	0	0:
74.	sf74	0:0	0:0	1:0:0	1:0	1:1	1:0	1	0	0:0	1	0:
75.	sf75	0:0	0:1	1:0:1	1:0	1:1	1:0	1	0	0:0	0	1:
76.	sf76	0:0	1:1	1:1:1	1:0	0:1	1:0	1	0	0:0	0	1:
77.	sf77	1:0	1:1	1:1:1	1:0	0:1	1:0	1	0	0:0	0	1:
78.	sf78	1:0	1:0	1:0:0	1:0	0:0	1:0	0	1	0:0	1	0:
79.	sf79	1:0	1:0	0:1:0	0:0	0:0	0:0	0	0	1:0	1	0:
80.	sf80	1:0	0:0	0:1:0	0:0	0:0	0:0	0	0	1:0	1	0:
81.	sf81	1:0	0:0	0:1:0	0:0	1:0	0:0	0	0	1:0	1	0:
82.	sf82	1:0	0:0	0:1:0	0:0	1:0	0:0	0	1	0:0	1	0:
83.	sf83	1:0	0:0	0:1:0	0:1	1:0	0:0	0	0	1:0	1	0:
84.	sf84	0:0	0:0	0:1:0	0:1	1:0	0:0	0	1	0:0	1	0:
85.	sf85	0:0	0:0	0:0:0	0:1	1:0	0:0	0	1	0:0	1	0:
86.	sf86	0:0	0:0	0:0:0	0:0	1:0	0:0	0	1	0:0	1	0:
87.	sf87	1:0	0:0	1:1:0	1:0	0:1	1:1	0	0	0:0	0	1:
88.	sf88	1:0	1:0	0:1:0	0:0	0:0	0:1	0	0	0:0	0	1:
89.	sf89	1:1	1:0	1:0:0	1:0	0:0	1:0	0	1	0:0	0	1:
90.	sf90	1:0	1:0	0:0:0	0:0	0:0	0:0	0	1	0:0	1	0:
91.	sf91	1:0	0:0	0:1:0	0:0	0:0	0:0	0	1	0:1	0	0:
92.	sf92	1:0	0:0	0:1:0	0:0	0:0	0:0	0	1	0:1	0	0:
93.	sf93	1:0	0:0	0:1:0	1:0	1:0	0:0	0	0	1:1	0	0:
94.	sf94	1:0	0:0	0:1:0	0:0	1:0	0:0	0	0	1:0	1	0:
95.	sf95	1:0	0:0	0:1:0	0:1	1:0	0:0	0	0	1:1	0	0:
96.	sf96	0:0	0:0	0:1:0	0:1	1:0	0:0	0	0	1:0	1	0:
97.	sf97	0:0	0:0	0:0:0	0:1	1:0	0:0	0	0	1:0	1	0:
98.	sf98	1:0	0:0	0:1:0	0:0	1:0	0:0	0	1	0:0	1	0:
99.	sf99	1:0	0:0	0:1:0	0:0	1:0	0:0	0	1	0:0	1	0:
100.	sf100	1:0	0:0	0:1:0	0:0	0:0	0:0	0	0	1:0	0	1:

To be continued...

Table 8. Continuation.

101.	sf101	1:0	0:0	0:1:0	0:0	0:0	0:0	0	1	0:0	1	0:
102.	sf102	1:0	0:0	0:1:0	0:0	0:0	0:0	0	1	0:1	0	0:
103.	sf103	1:0	0:0	0:1:0	0:0	0:0	0:0	0	0	1:1	0	0:
104.	sf104	1:0	0:0	0:1:0	1:0	1:0	0:0	0	1	0:0	1	0:
105.	sf105	1:0	0:0	0:1:0	0:0	1:0	0:0	0	1	0:1	0	0:
106.	sf106	1:0	0:0	0:1:0	0:1	1:0	0:0	0	0	1:0	1	0:
107.	sf107	0:0	0:0	0:1:0	0:1	1:0	0:0	0	1	0:0	1	0:
108.	sf108	1:0	0:0	0:1:0	0:1	1:0	0:0	0	0	1:1	0	0:
109.	sf109	1:0	0:0	0:1:0	0:0	1:0	0:0	0	1	0:0	1	0:
110.	sf110	1:1	1:0	0:0:0	0:0	0:0	0:0	0	1	0:0	1	0:
111.	sf111	1:0	0:0	0:0:0	0:0	0:0	0:0	0	1	0:1	0	0:
112.	sf112	1:0	0:0	0:1:0	0:0	0:0	0:0	0	0	1:1	0	0:
113.	sf113	1:0	0:0	0:0:0	0:0	0:0	0:0	0	1	0:0	1	0:
114.	sf114	1:0	0:0	0:1:0	0:0	1:0	0:0	0	1	0:0	1	0:
115.	sf115	1:0	0:0	0:0:0	0:0	1:0	1:0	0	1	0:0	1	0:
116.	sf116	0:0	0:0	0:0:0	0:1	1:0	0:0	0	1	0:0	1	0:
117.	sf117	1:0	0:0	0:1:0	0:1	1:0	0:0	0	0	1:0	1	0:
118.	sf118	1:0	0:0	0:1:0	0:1	1:0	0:0	0	0	1:1	0	0:
119.	sf119	1:1	1:0	0:0:0	0:0	0:0	0:0	0	1	0:0	1	0:
120.	sf120	1:0	0:0	0:0:0	0:0	0:0	0:0	0	1	0:1	0	0:
121.	sf121	1:0	0:0	0:1:0	1:0	0:0	1:0	0	1	0:1	0	0:
122.	sf122	1:0	0:0	1:0:0	1:0	0:1	1:1	0	0	0:0	1	0:
123.	sf123	1:0	0:0	1:0:0	1:0	1:0	1:0	0	1	0:0	1	0:
124.	sf124	1:0	0:0	0:1:0	0:0	1:0	0:0	0	0	1:0	1	0:
125.	sf125	1:0	0:0	0:0:0	0:1	1:0	0:0	0	1	0:1	0	0:
126.	sf126	1:0	0:0	0:0:0	0:1	1:0	0:0	0	1	0:1	0	0:
127.	sf127	1:1	1:0	0:0:0	0:0	0:0	1:0	0	1	0:0	1	0:
128.	sf128	1:0	0:0	0:1:0	1:0	0:0	0:0	0	1	0:0	1	0:
129.	sf129	1:0	1:0	1:1:0	1:0	0:0	1:0	0	1	0:1	0	0:
130.	sf130	1:0	1:0	1:0:0	1:0	0:0	1:0	0	1	0:0	1	0:
131.	sf131	1:1	1:0	1:1:0	0:0	1:0	0:0	0	1	0:0	1	0:
132.	sf132	1:0	1:0	0:0:0	0:0	1:0	1:0	0	1	0:0	1	0:
133.	sf133	1:0	0:0	0:0:0	0:1	1:0	1:0	0	1	0:0	1	0:

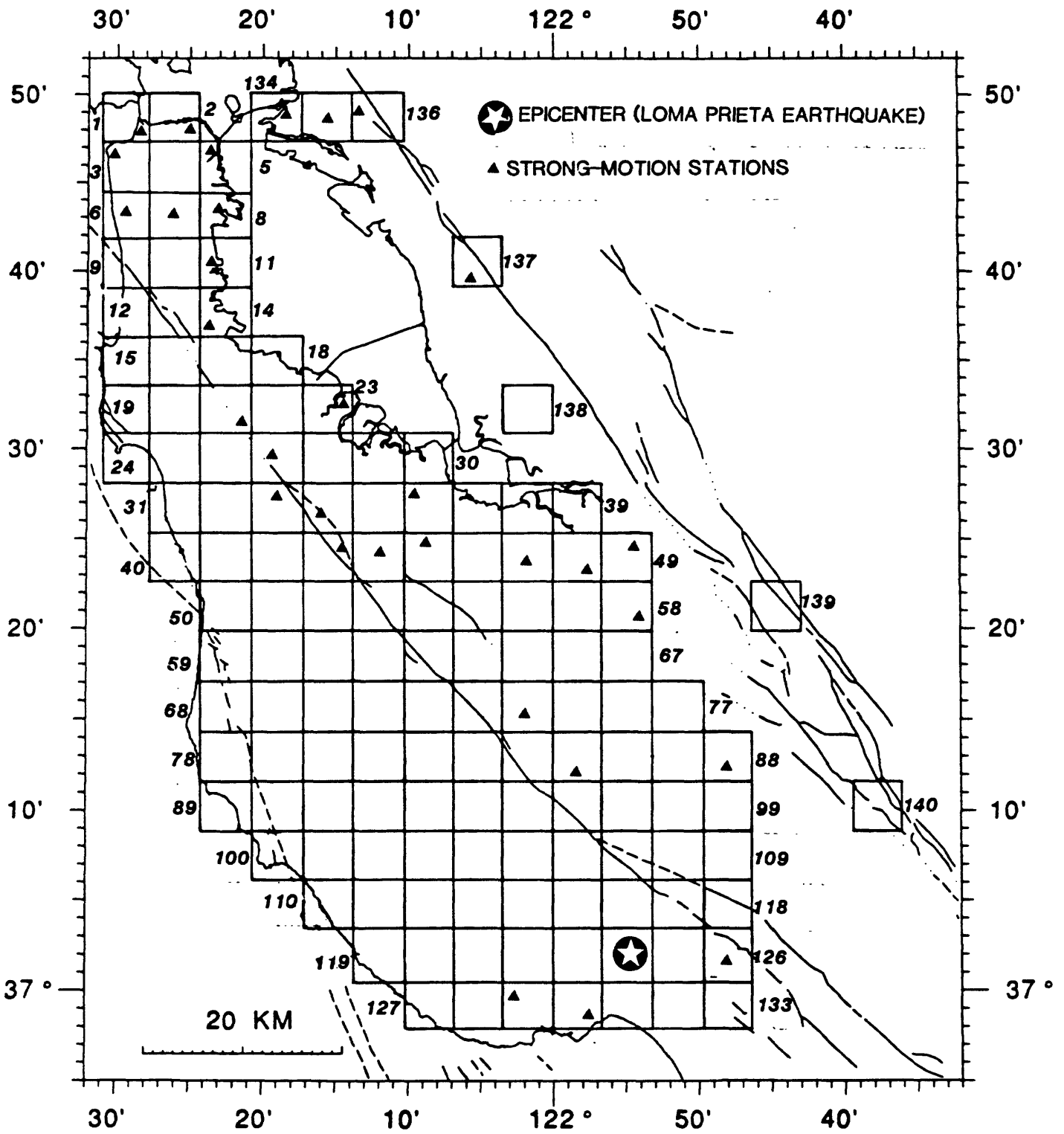


Figure 1. The area under study and elements considered (1-140 are the numbers of elements).

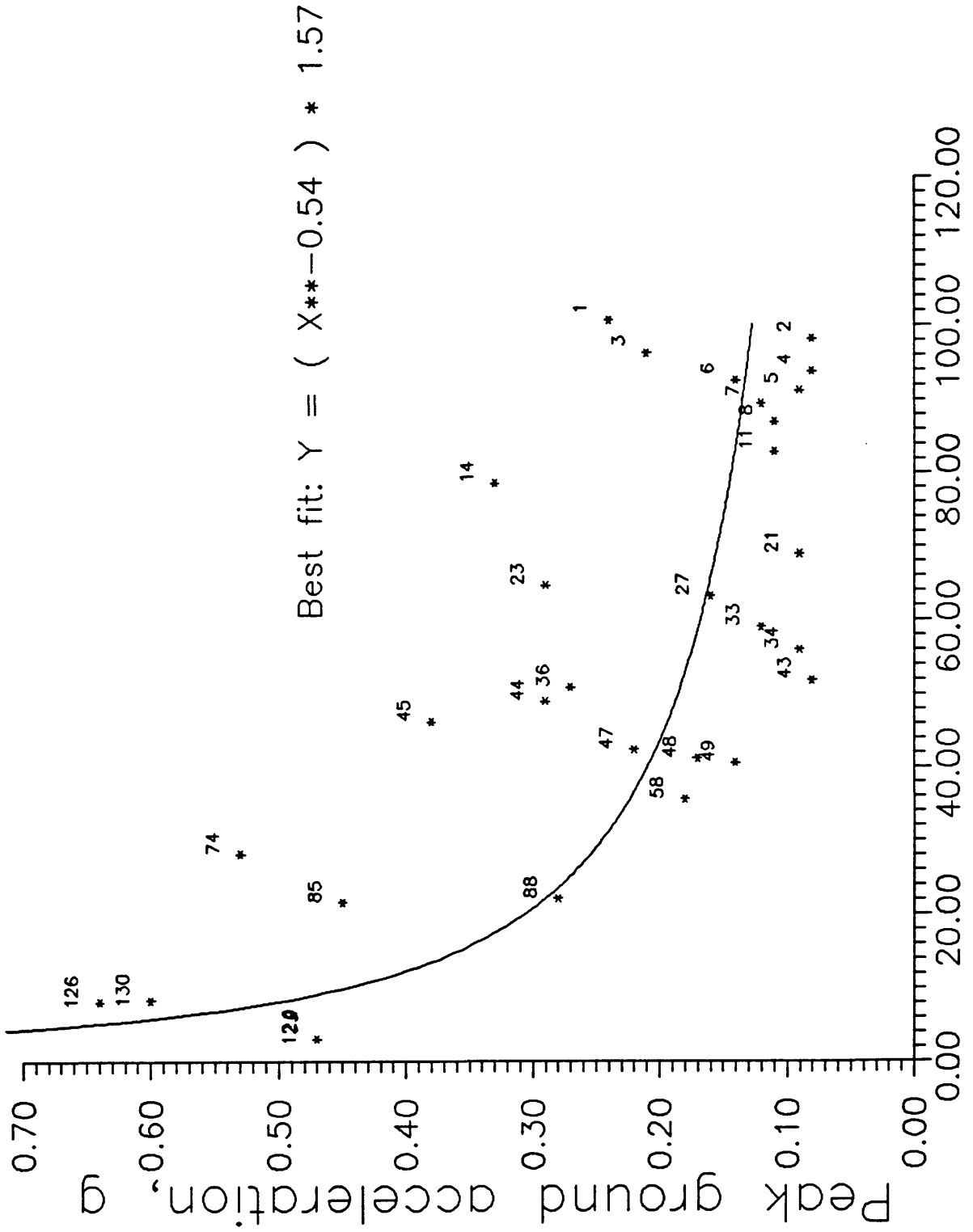


Figure 2. Relationship between epicentral distance and peak ground acceleration (PGA)

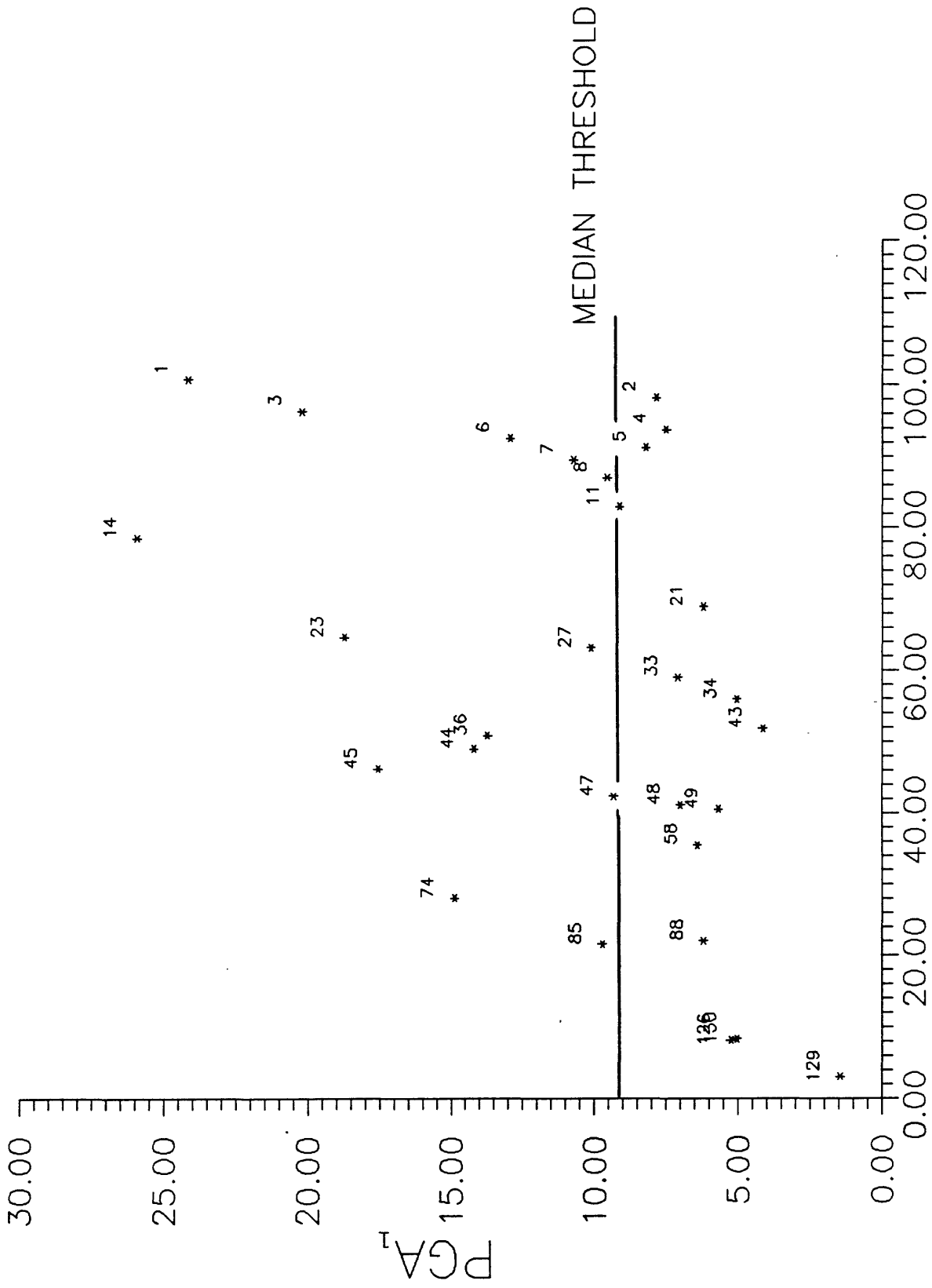


Figure 3. Relationship between epicentral distance and calculated characteristic, PGA1.

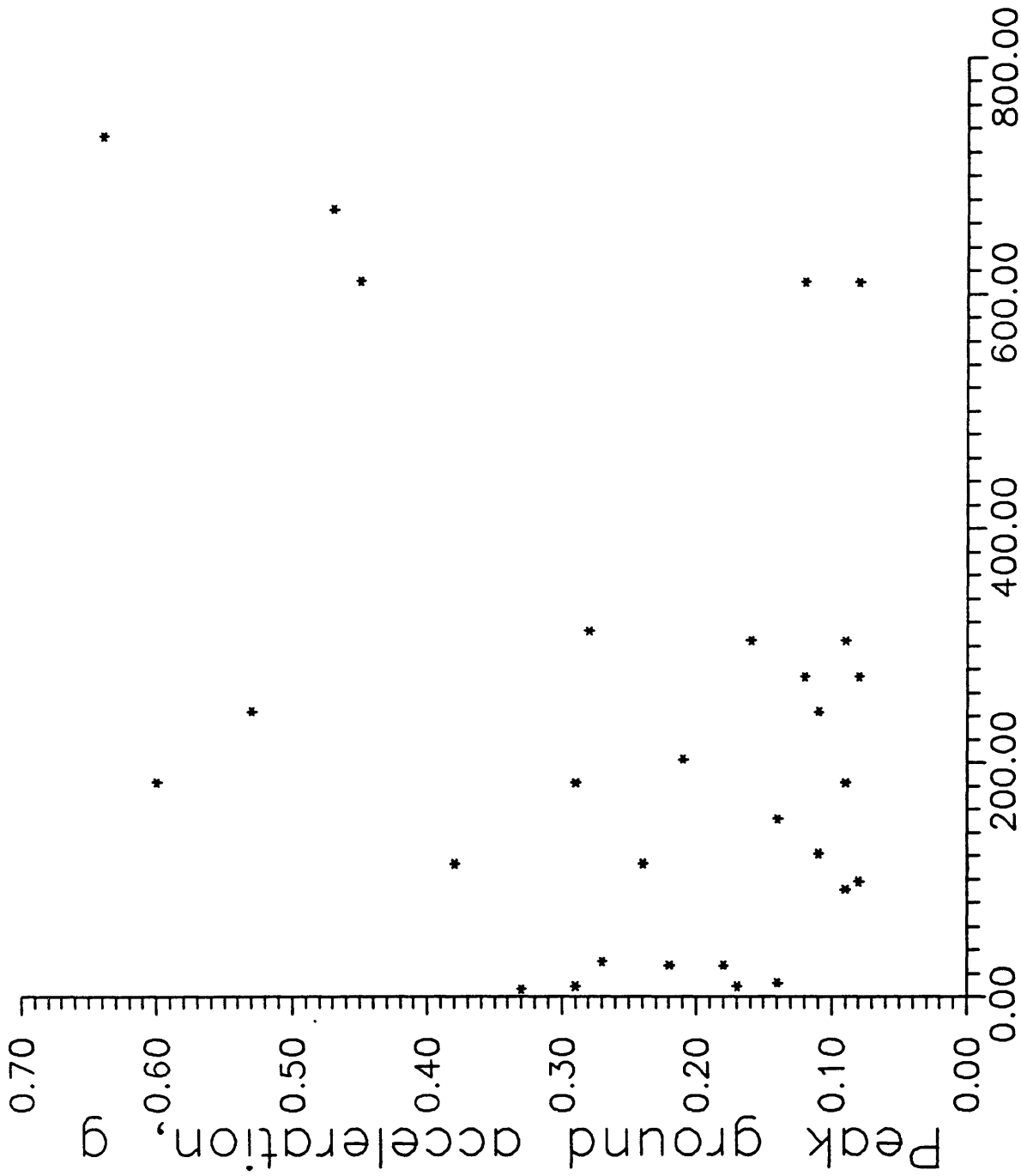


Figure 4. Relationship between peak ground acceleration (PGA) and maximum elevations within elements.

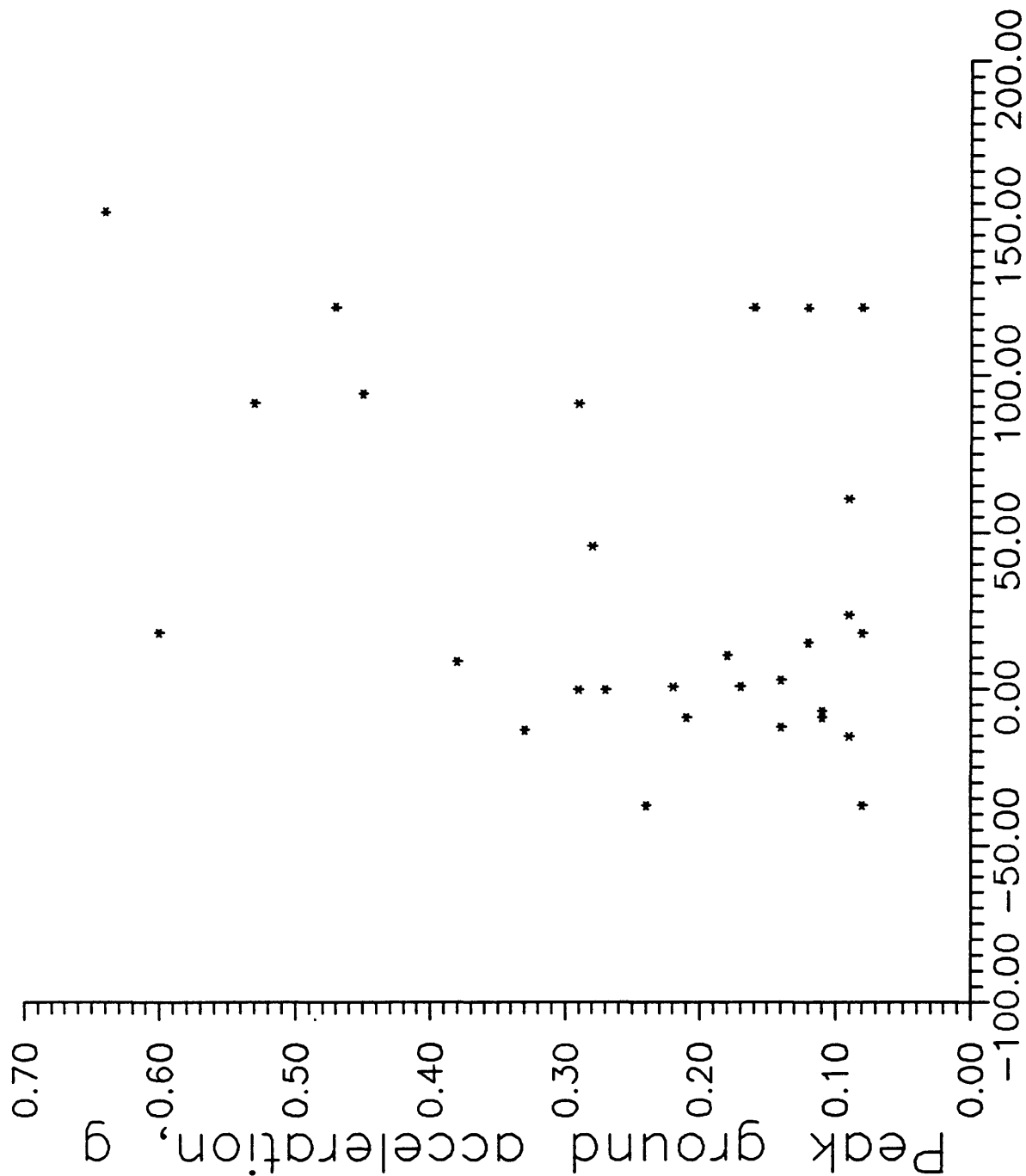


Figure 5. Relationship between peak ground acceleration (PGA) and minimum elevations within elements.

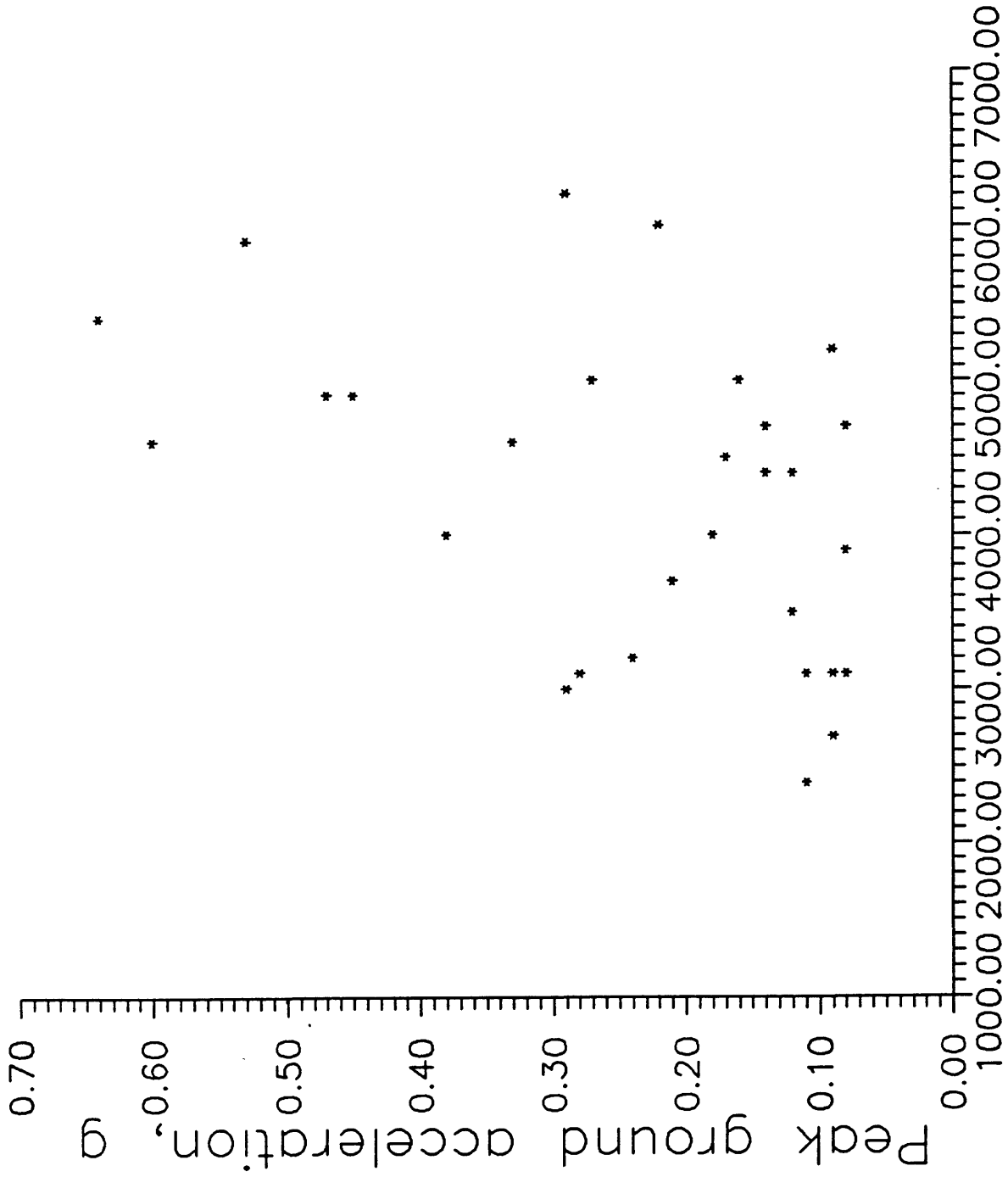


Figure 6. Relationship between peak ground acceleration (PGA) and distance between points of maximum and minimum elevations.

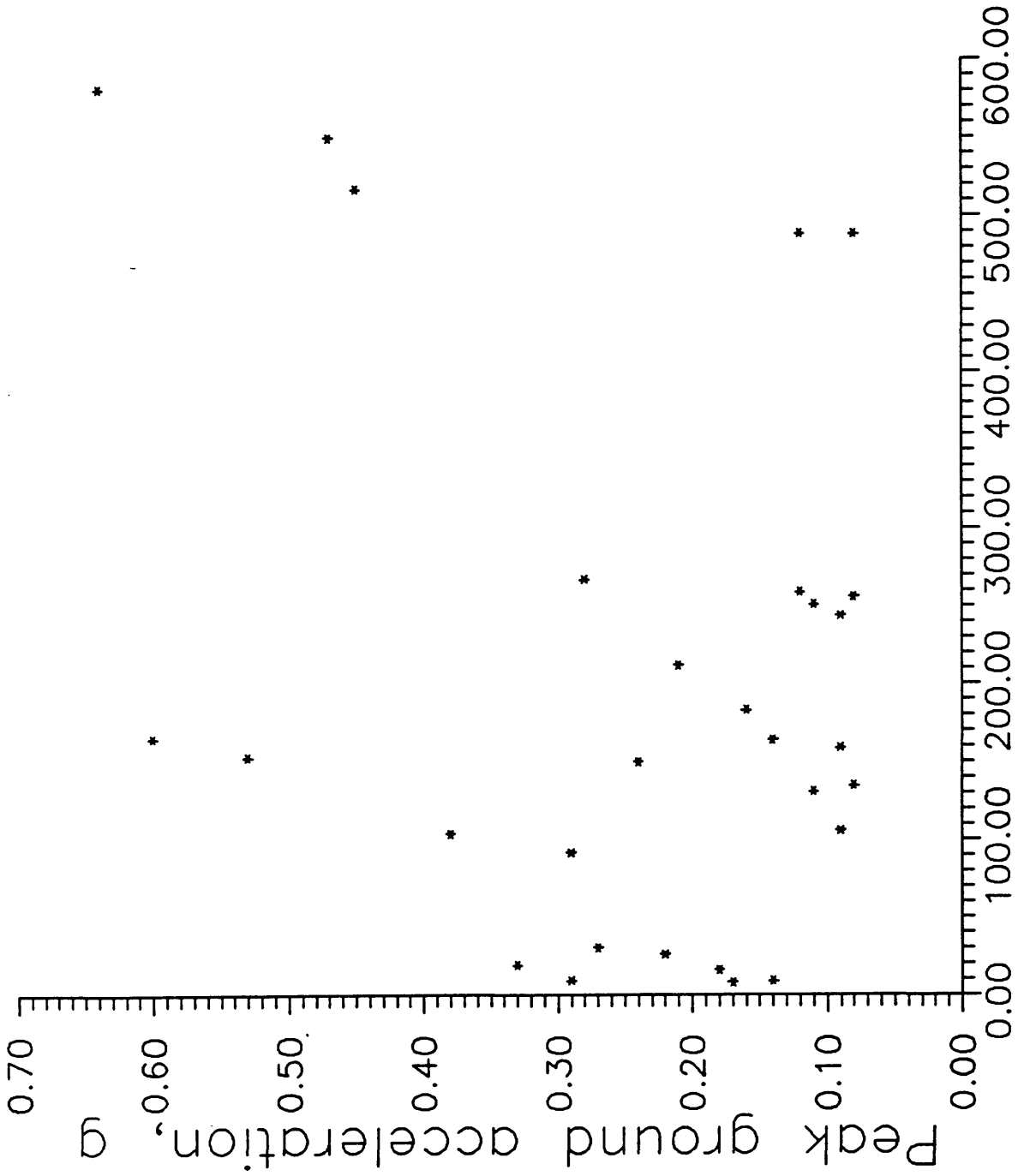


Figure 7. Relationship between peak ground acceleration (PGA) and difference of maximum and minimum elevations.

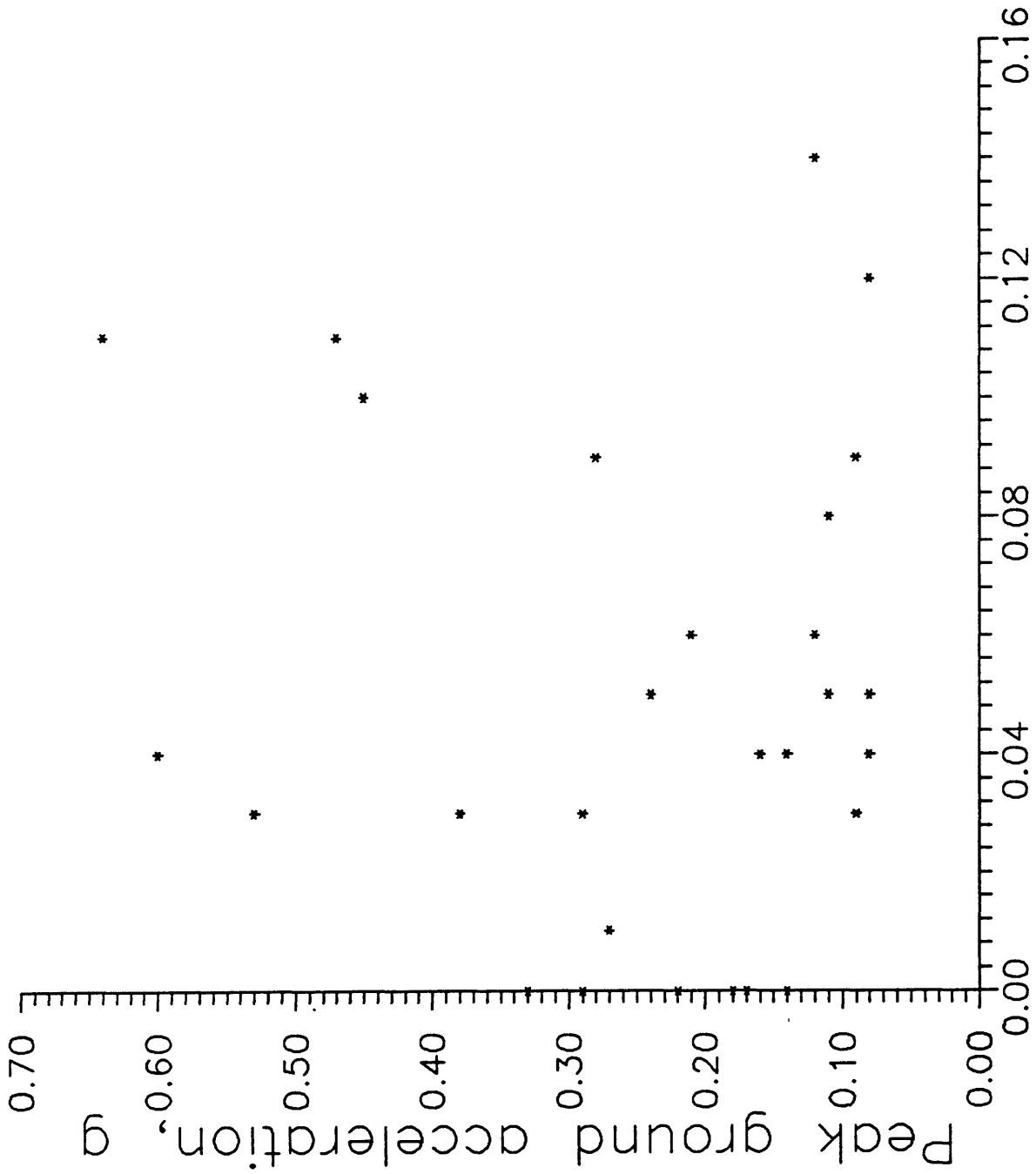


Figure 8. Relationship between peak ground acceleration (PGA) and topographic gradient.

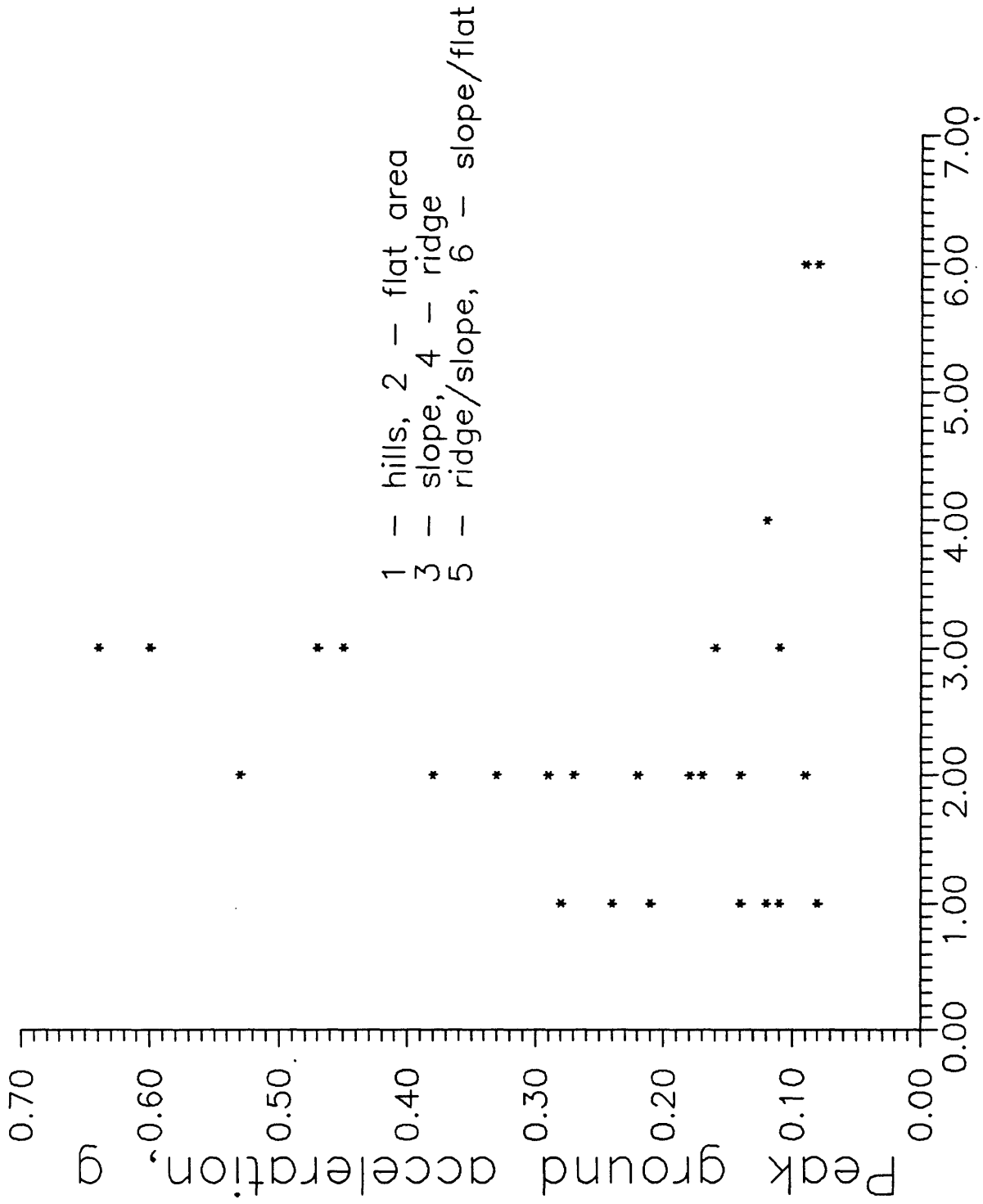


Figure 9. Relationship between peak ground acceleration (PGA) and landforms.

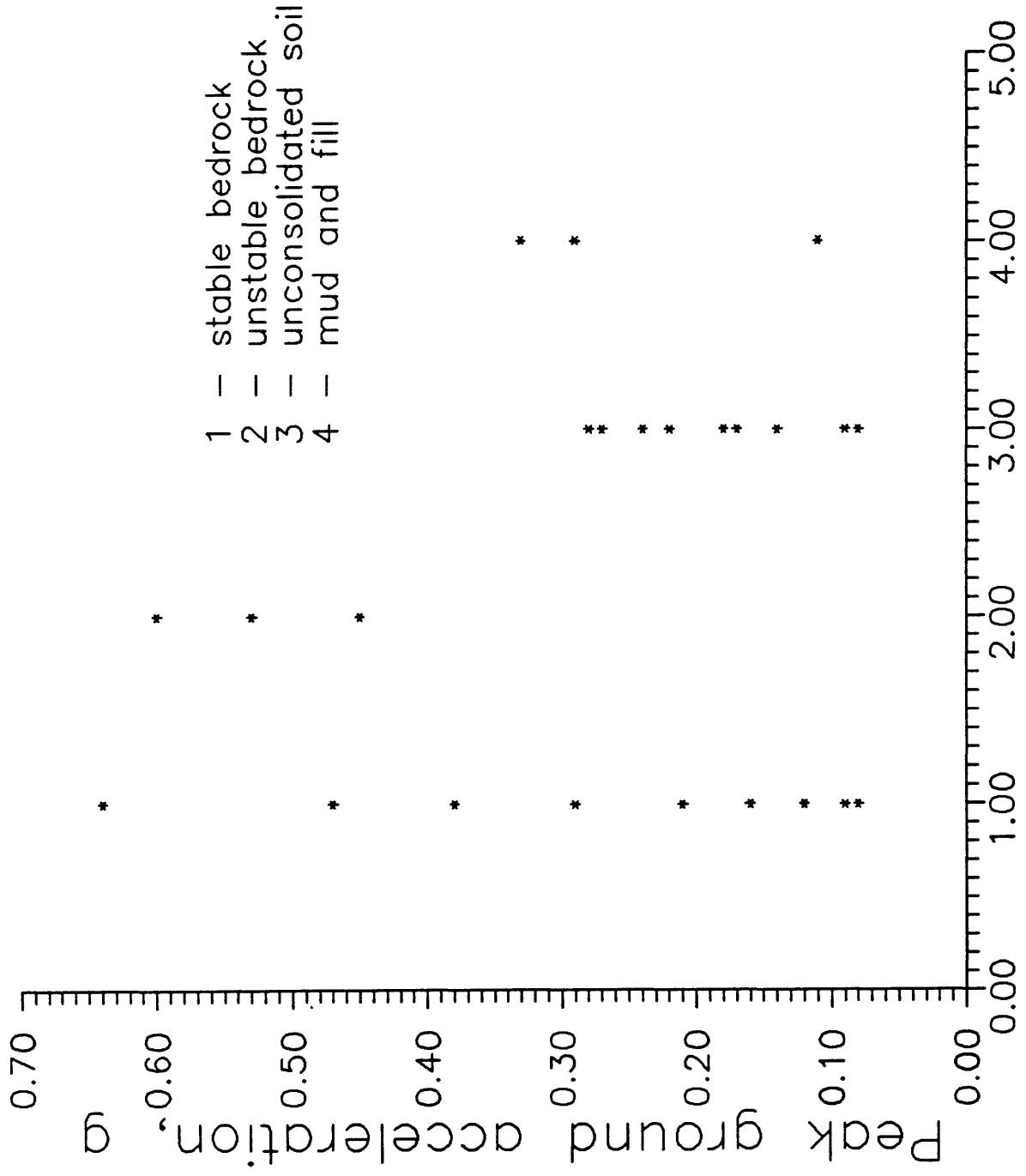


Figure 10. Relationship between peak ground acceleration (PGA) and soil types.

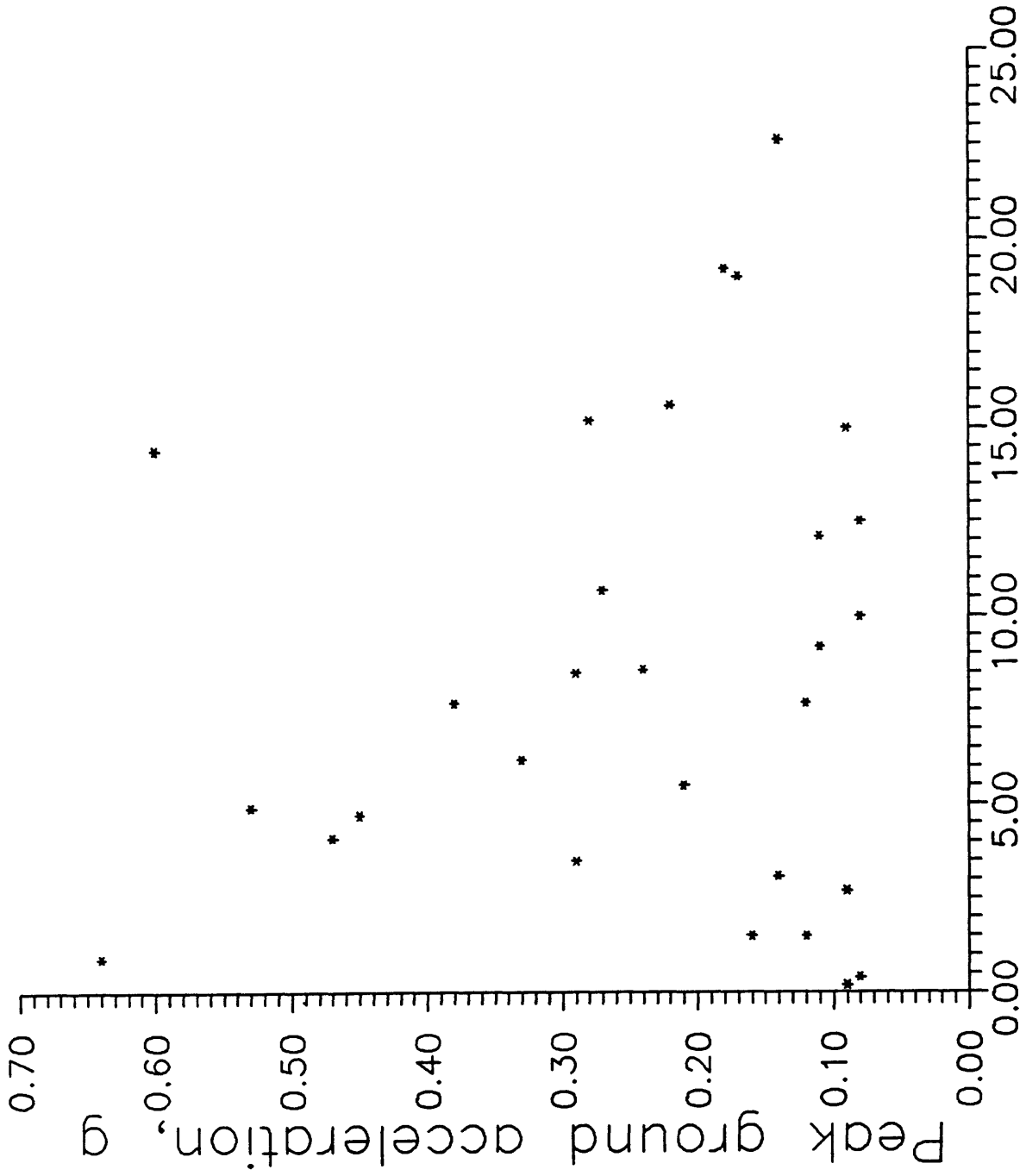


Figure 11. Relationship between peak ground acceleration (PGA) and shortest distance to San Andreas fault.

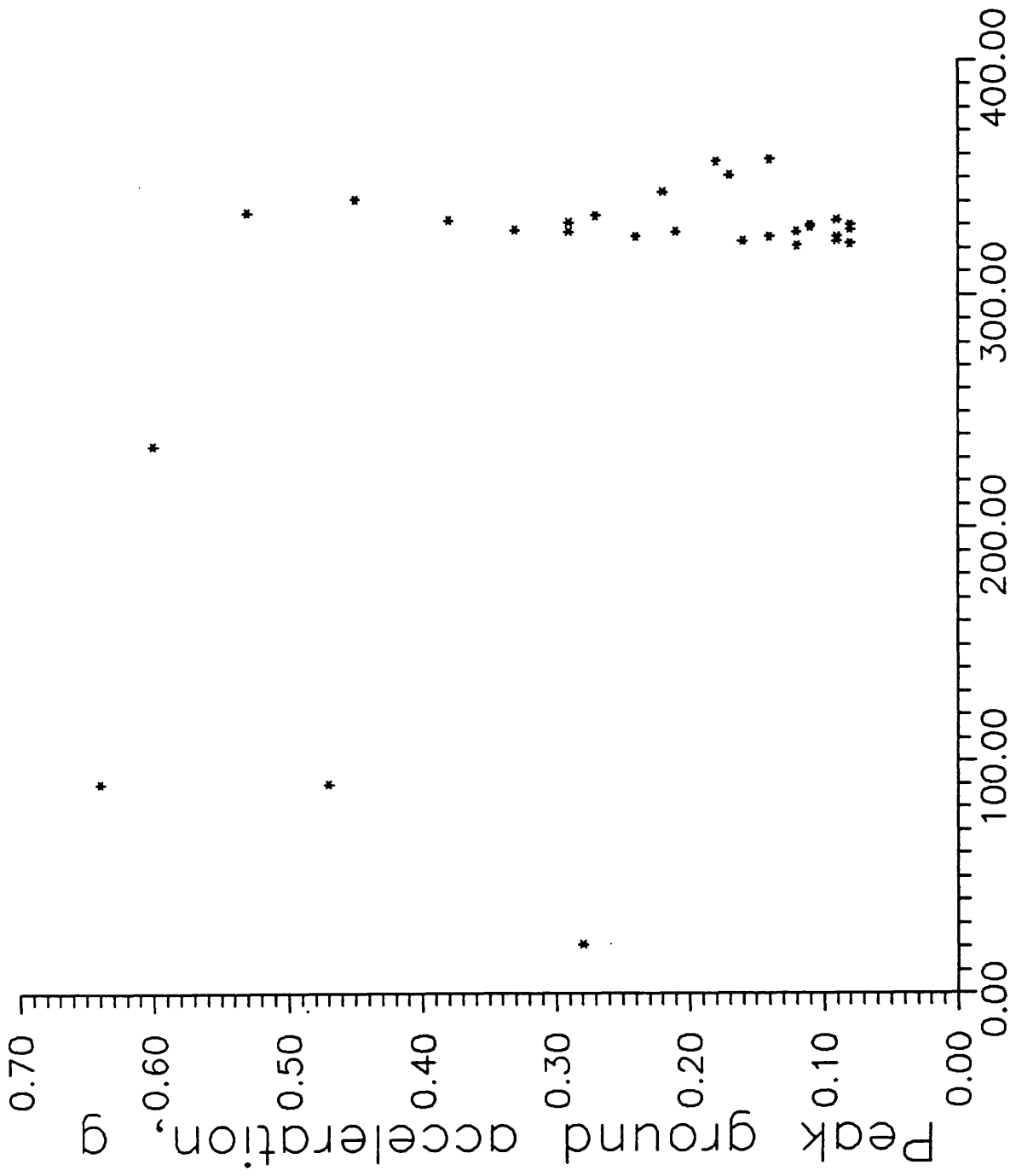


Figure 12. Relationship between peak ground acceleration (PGA) and azimuth to the epicenter.

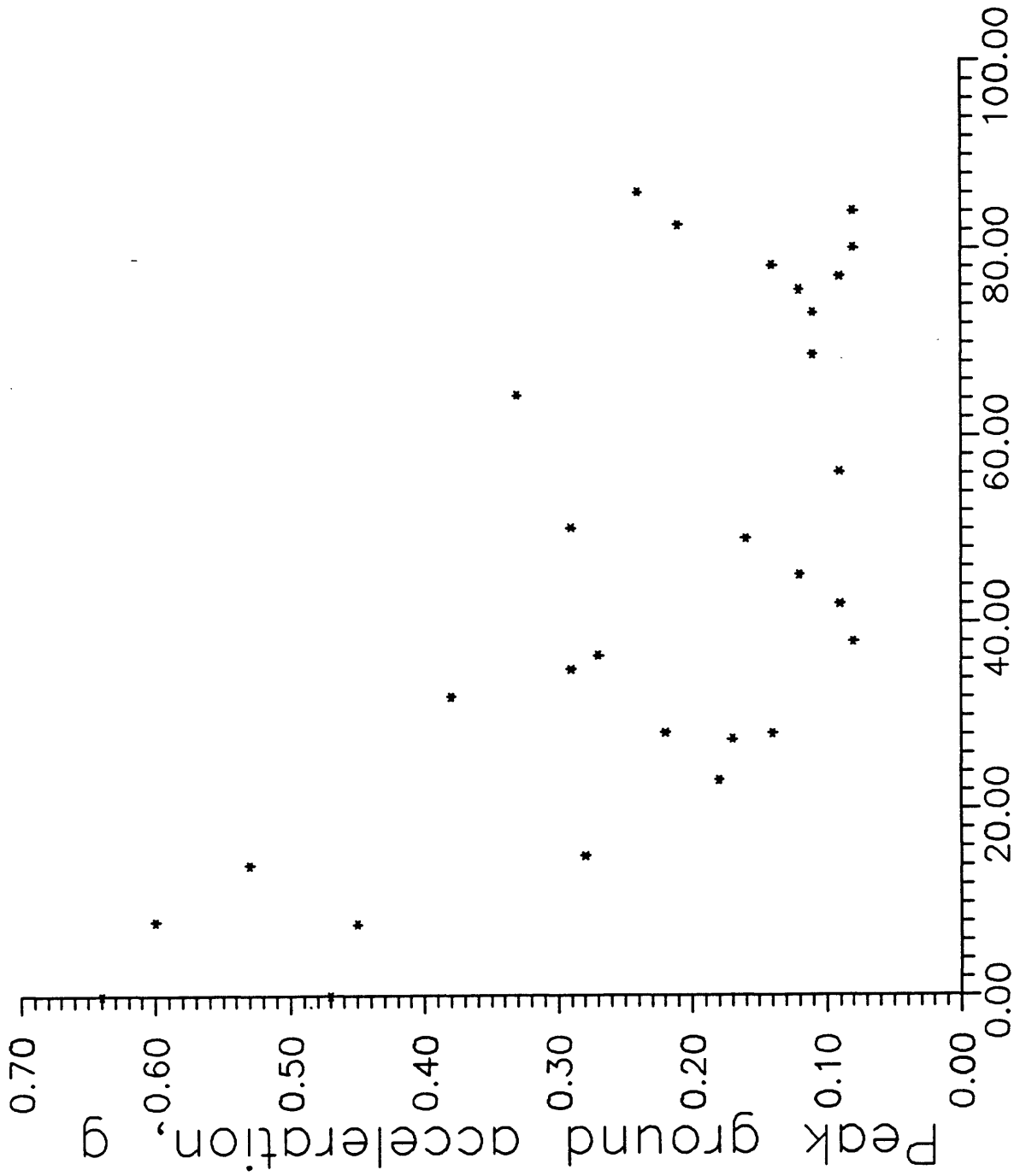


Figure 13. Relationship between peak ground acceleration (PGA) and shortest distance to the rupture zone.

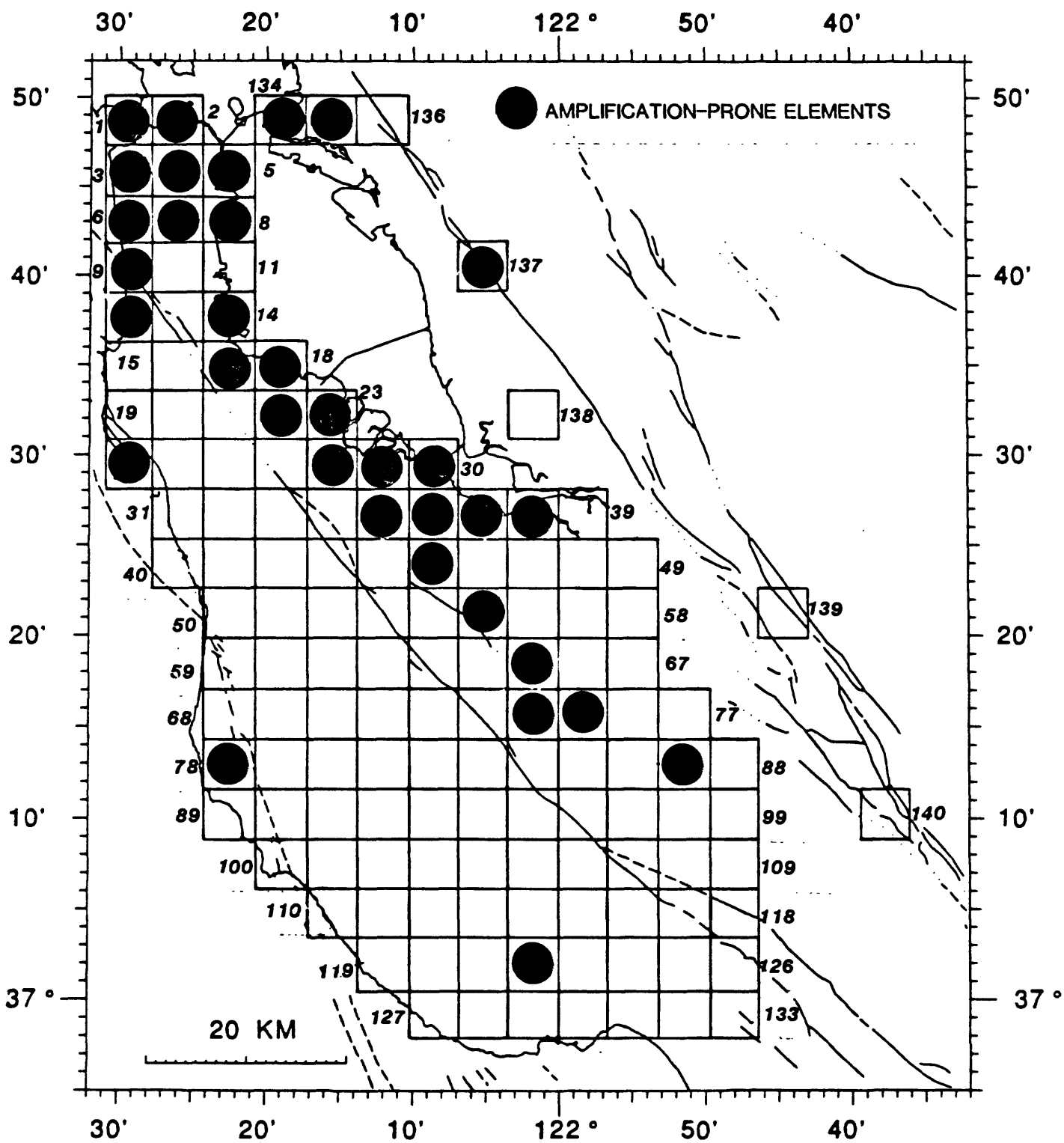


Figure 14. Elements recognized as amplification-prone.